



# BRNO UNIVERSITY OF TECHNOLOGY

VYSOKÉ UČENÍ TECHNICKÉ V BRNĚ

## FACULTY OF CHEMISTRY

FAKULTA CHEMICKÁ

## INSTITUTE OF CHEMISTRY AND TECHNOLOGY OF ENVIRONMENTAL PROTECTION

ÚSTAV CHEMIE A TECHNOLOGIE OCHRANY ŽIVOTNÍHO PROSTŘEDÍ

## NEW TANDEM METHODS OF WATER TREATMENT USING ELECTROCHEMICAL OXIDATION AND PHOTOCATALYSIS FOR THE DEGRADATION OF MICROPOLLUTANTS

NOVÉ TANDEMOVÉ METODY ÚPRAVY VODY POMOCÍ ELEKTROCHEMICKÉ OXIDACE A FOTOKATALÝZY PRO DEGRADACI MIKROPOLUTANTŮ

### MASTER'S THESIS

DIPLOMOVÁ PRÁCE

### AUTHOR

AUTOR PRÁCE

Bc. Dominika Čičatková

### SUPERVISOR

VEDOUCÍ PRÁCE

RNDr. Veronika Ostatná, Ph.D.

BRNO 2025

# Assignment Master's Thesis

Project no.: FCH-DIP2117/2024 Academic year: 2024/25  
Department: Institute of Chemistry and Technology  
of Environmental Protection  
Student: **Bc. Dominika Čičatková**  
Study programme: Environmental Sciences and  
Engineering  
Field of study: no specialisation  
Head of thesis: **RNDr. Veronika Ostatná, Ph.D.**

## Title of Master's Thesis:

New tandem methods of water treatment using electrochemical oxidation and photocatalysis for the degradation of micropollutants

## Master's Thesis:

Development of wastewater treatment based on tandem degradation of organic micropollutants by light by controlled generation of reactive oxygen species using photocatalysts derived from of bio-inspired organic molecules and electrochemical anodic oxidation on carbon electrodes

## Deadline for Master's Thesis delivery: 5.5.2025:

Master's Thesis should be submitted to the institute's secretariat in a number of copies as set by the dean This specification is part of Master's Thesis

-----  
Bc. Dominika Čičatková  
student

RNDr. Veronika Ostatná, Ph.D.  
Head of thesis

prof. Ing. Jozef Krajčovič, Ph.D.  
Head of department

In Brno dated 3.2.2025

-----  
prof. Ing. Michal Veselý, CSc.  
Dean

## **ABSTRAKT**

Tato diplomová práce představuje výsledky, které mohou sloužit jako základ pro vývoj nové tandemové metody čištění odpadních vod, založené na kombinaci elektrochemické oxidace a fotokatalýzy. Tento přístup spadá do kategorie pokročilých oxidačních procesů určených k degradaci organických mikropolutantů. Práce se zaměřuje na rozklad modelové sloučeniny, methylenové modři, pomocí dvou separátních degradačních mechanismů: elektrochemické oxidace a fotokatalytické produkce reaktivních forem kyslíku za využití organických bio-fotokatalyzátorů. V práci jsou využívány materiály jako grafitová tuha sloužící jako pracovní elektroda a nově syntetizovaný flavinový derivát A-Na-TEG jako bio-fotokatalyzátor. Tyto materiály představují ekonomicky výhodné a environmentálně udržitelné řešení pro čištění odpadních vod. Výsledky prokázaly účinnou degradaci methylenové modři jak elektrolytickým procesem, tak prostřednictvím reaktivních forem kyslíku generovaných fotokatalyzátorem. Kombinace obou přístupů naznačuje potenciál pro efektivní implementaci tandemové metody čištění.

## **ABSTRACT**

This master's thesis presents results that could serve as a foundation for the development of a new tandem method for wastewater treatment, based on the combination of electrochemical oxidation and photocatalysis. This approach falls under the category of advanced oxidation processes aimed at the degradation of organic micropollutants. The study focuses on the breakdown of a model compound, methylene blue, using two separate degradation mechanisms: electrochemical oxidation and the photocatalytic generation of reactive oxygen species using organic bio-photocatalysts. Materials such as graphite pencils as working electrodes and a newly synthesized flavin derivative, A-Na-TEG, as the bio-photocatalyst were employed. These materials offer an economically viable and environmentally sustainable solution for wastewater treatment. The results demonstrated successful degradation of methylene blue through both electrolysis and reactive oxygen species generated by the photocatalyst. The effective integration of both approaches shows strong potential for the implementation of a tandem treatment method.

## **KLÍČOVÁ SLOVA**

Mikropolutanty; odpadní voda; elektrochemická oxidace; fotokatalýza; reaktivní formy kyslíku; bio-fotokatalyzátor; methylenová modř; tandemová metoda

## **KEYWORDS**

Micropollutants; wastewater; electrochemical oxidation; photocatalysis; reactive oxygen species; bio-photocatalyst; methylene blue; tandem method

### **CITATION OF THE PRINTED VERSION**

ČIČATKOVÁ, Dominika. Nové tandemové metody úpravy vody pomocí elektrochemické oxidace a fotokatalýzy pro degradaci mikropolutantů. Brno, 2024. Dostupné také z: <https://www.vut.cz/studenti/zav-prace/detail/162085>. Diplomová práce. Vysoké učení technické v Brně, Fakulta chemická, Ústav chemie a technologie ochrany životního prostředí. Vedoucí práce Veronika Ostatná.

### **CITATION OF THE ELECTRONIC VERSION**

ČIČATKOVÁ, Dominika. Nové tandemové metody úpravy vody pomocí elektrochemické oxidace a fotokatalýzy pro degradaci mikropolutantů [online]. Brno, 2024 [cit. 2024-08-21]. Dostupné z: <https://www.vut.cz/studenti/zav-prace/detail/162085>. Diplomová práce. Vysoké učení technické v Brně, Fakulta chemická, Ústav chemie a technologie ochrany životního prostředí. Vedoucí práce Veronika Ostatná.

### **DECLARATION**

I declare that the master's thesis has been worked out by myself and that all the quotations from the used literary sources are accurate and complete. The content of the master's thesis is the property of the Faculty of Chemistry of Brno University of Technology, and all commercial uses are allowed only if approved by both the supervisor and the dean of the Faculty of Chemistry, BUT.

.....  
Bc. Dominika Čičatková

## **ACKNOWLEDGEMENT**

I would like to express my sincere gratitude to my master's thesis supervisor, RNDr. Veronika Ostatná, Ph.D., for her professional guidance, patience and support throughout the development of this thesis.

My special thanks also go to RNDr. Hana Černocká, Dr., from the Institute of Biophysics of the Czech Academy of Sciences, for her assistance during the experimental part of this work.

I am grateful to my co-supervisor, Dr. Mathilde Knott, from Rheinland-Pfälzische Technische Universität Kaiserslautern-Landau, for her mentorship.

I would like to extend my appreciation to prof. Ing. Jozef Krajčovič, Ph.D., from the Faculty of Chemistry at Brno University of Technology, for facilitating of the collaboration with the Institute of Biophysics, and to Ing. Lucia Ivanová, Ph.D., also from the Faculty of Chemistry, for providing the synthesized flavin essential for this thesis.

Last but not least, I would like to thank my family and my partner for their constant encouragement, understanding, and support throughout my studies.

## TABLE OF CONTENTS

|   |    |
|---|----|
| 1. INTRODUCTION.....  | 8  |
| 2. THEORETICAL PART .....                                     | 9  |
| 2.1 Background on wastewater treatment and MPs .....          | 9  |
| 2.2 Theoretical background on AOPs.....                       | 11 |
| 2.3 Electrochemical systems .....                             | 15 |
| 2.3.1 Working electrodes .....                                | 16 |
| 2.3.2 Reference electrodes .....                              | 18 |
| 2.3.3 Auxiliary electrodes.....                               | 19 |
| 2.4 Electrode   electrolyte interface .....                   | 19 |
| 2.5 Principles of AO .....                                    | 21 |
| 2.6 Electrochemical methods .....                             | 22 |
| 2.6.1 Cyclic voltammetry .....                                | 22 |
| 2.6.2 Square wave voltammetry .....                           | 24 |
| 2.6.3 Chronoamperometry.....                                  | 25 |
| 2.7 Photocatalysis as an advanced water treatment method..... | 26 |
| 2.8 Molecular Spectroscopy .....                              | 28 |
| 2.8.1 UV-VIS Spectrophotometry .....                          | 29 |
| 2.9 Chemistry of the MB.....                                  | 32 |
| 2.10 Chemistry of the Flavin.....                             | 32 |
| 3. EXPERIMENTAL PART .....                                    | 34 |
| 3.1 Chemicals .....   | 34 |
| 3.2 Equipment .....   | 34 |
| 3.3 Preparation of working solutions .....                    | 35 |
| 3.4 Apparatus for electrochemical analysis.....               | 35 |
| 3.5 Frequency optimization.....                               | 36 |
| 3.6 Chronoamperometric measurement .....                      | 36 |
| 3.7 Modification of the electrode surface.....                | 37 |
| 3.8 Photocatalytic measurement.....                           | 38 |
| 4. RESULTS AND DISCUSSION .....                               | 39 |
| 4.1 Electrochemical degradation of MB.....                    | 39 |
| 4.1.1 Frequency dependence .....                              | 40 |
| 4.1.2 Concentration dependence .....                          | 41 |

|  |    |
|--|----|
| 4.1.3 Modification of the working electrode surface .....        | 42 |
| 4.1.4 Electrolysis of the MB solution using unmodified PGE ..... | 44 |
| 4.1.5 Electrolysis of the MB solution using modified PGE .....   | 45 |
| 4.2 Photocatalytic degradation of MB.....                        | 48 |
| 5. CONCLUSION .....  | 50 |
| 6. REFERENCES.....   | 51 |
| 7. LIST OF ABBREVIATIONS .....                                   | 59 |

## 1. INTRODUCTION

Water is the most important substance for life on Earth, so its quality and accessibility are very important. Water use is linked to water pollution caused by uncontrolled anthropogenic activities. The problem is that human activity often includes contamination of water with highly toxic and persistent substances which can remain for long time in the environment. As the social economy rapidly develops, the widespread presence of micropollutants (MPs) - including pharmaceuticals, personal care products, endocrine-disrupting chemicals, pesticides, and perfluorinated alkylated substances - in wastewater has increasingly exacerbated water scarcity by compromising water quality [1; 2].

In general, MPs are found in low concentrations from ng/L to µg/L in aquatic environments, making them challenging to eliminate in wastewater treatment plants (WWTPs). Even at these low levels, MPs can disrupt the endocrine systems of organisms, and the physical, chemical, and biological processes used in treatment plants are not fully effective at removing them. Negative effects that can be caused by MPs include reproductive and sexual abnormalities, reduced sperm counts, neurological disorders, and a higher risk of testicular, prostate, ovarian, and breast cancers [2].

Recent scientific findings have led to several EU Commission strategies emphasizing the need to address MPs, which are now routinely detected in all waters across the European Union. Primary, secondary, and tertiary treatments remove some MPs, however quaternary treatment is needed to address a wider range, focusing on organic MPs with existing removal technologies. Its implementation should follow the precautionary principle and a risk-based approach.

All urban WWTPs serving 150 000 population equivalent (PE) or more should implement quaternary treatment, as these facilities account for a significant portion of micropollutant discharges, and removal at this scale is cost-effective. Member States should prioritize investments in these plants, ensuring those posing the greatest risks to the environment and human health are upgraded promptly. Additionally, for agglomerations of 10 000 PE or more, quaternary treatment should be mandatory in areas sensitive to micropollutant pollution. According to the EU Parliament and the Council, to allow Member States sufficient time to plan and implement the necessary infrastructure, the requirement for quaternary treatment should be introduced gradually, with clear interim targets, and fully applied by 2045 [3].

In recent decades, advanced oxidation processes (AOPs) have attracted considerable attention due to their high efficiency, low production of secondary pollutants, minimal space requirements, and excellent environmental compatibility. These attributes position AOPs as a promising technology for next-generation wastewater treatment. Anodic oxidation (AO) and photocatalysis, a key AOPs, involve oxidation reactions, which convert contaminants into smaller molecules or even fully mineralize them into carbon dioxide (CO<sub>2</sub>) and water through direct and indirect oxidation processes [2; 4; 5; 6].

## 2. THEORETICAL PART

### 2.1 Background on wastewater treatment and MPs

As global water demand continues to rise, wastewater treatment becomes essential for maintaining water quality. However, traditional treatment methods are increasingly ineffective at addressing modern pollutants, particularly MPs, which pose significant risks to both ecosystems and human health.

Wastewater originates from various sources, each contributing distinct contaminants. Domestic wastewater comes from homes, schools, and businesses. Industrial wastewater is generated by manufacturing processes, such as those in the pharmaceutical or food industries. Infiltration and inflow occur when water enters the sewer system through leaks or groundwater. Municipal wastewater is typically collected in sanitary sewers and transported to WWTPs, while stormwater is usually handled by separate storm sewers. Industrial wastewater is often treated onsite or pretreated before being discharged into sanitary sewers [7; 8].

To address these diverse sources of wastewater, treatment is typically carried out in three stages: primary, secondary, and tertiary treatment. The primary treatment stage focuses on removing coarse impurities through screens, primarily serving as protection for the plant's equipment. This is followed by sedimentation in a primary settling tank, where suspended solids containing high levels of biochemical oxygen demand (BOD<sub>5</sub>) are separated. A coagulant is usually added to aid the aggregation of suspended solids into flocs.

The secondary treatment stage involves biological treatment, where microorganisms break down organic matter into simpler substances in activation tanks. The effectiveness of secondary treatment is measured by the reduction in BOD<sub>5</sub> and suspended solids. After this stage, the water is sent to a settling tank for further sedimentation.

While secondary treatment is commonly considered as the final stage before discharge into water recipients, such as rivers or streams, the tertiary stage is increasingly utilized for additional treatment. This stage often involves activated carbon adsorption or membrane processes like microfiltration or ultrafiltration, which remove colloidal substances, macromolecules, bacteria, and even viruses from treated water [7; 9]. Brief overview of wastewater treatment stages can be seen in Figure 1.

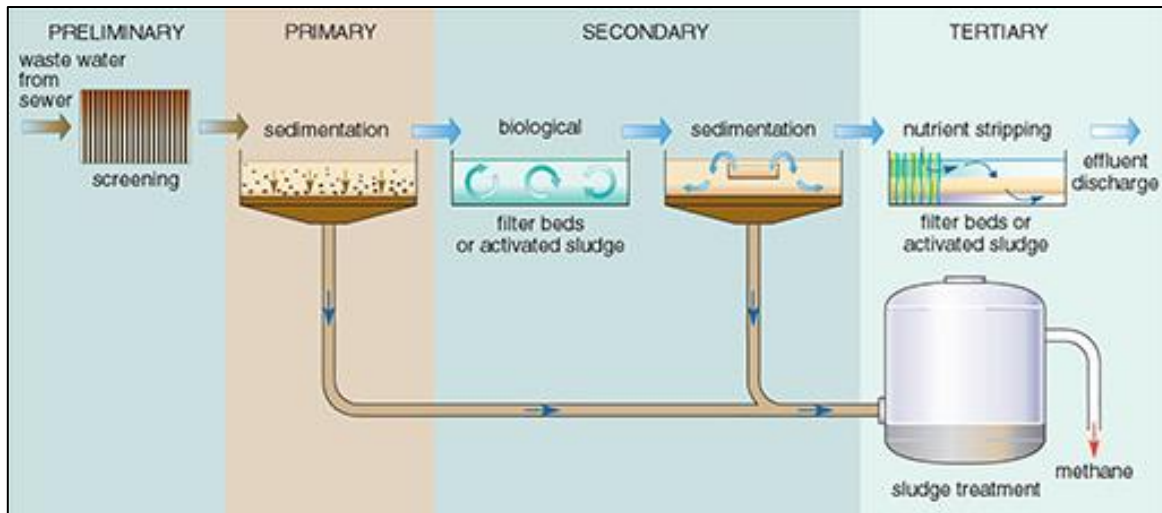


Figure 1 Overview of wastewater treatment stages [10]

The main indicators that have been a focus for removal from wastewater over the past decades include total organic carbon (TOC), total nitrogen ( $N_{\text{total}}$ ), and total phosphorus ( $P_{\text{total}}$ ). The maximum allowable limits for these substances in treated wastewater depend on the wastewater regulations of each country. In the Czech Republic, these limits are specified in the Water Act No. 254/2001 Coll [8; 11].

While WWTPs efficiently remove conventional pollutants, they remain a primary source of MP discharge into the environment. These substances, including pharmaceuticals and personal care products (PPCPs), biocides, pesticides, and various other chemicals commonly used in households and industry, are collectively referred to as MPs. Their persistence in the environment and potential harm to human health present new challenges for wastewater treatment systems [11; 9].

Due to the vast diversity of MPs, there is currently limited information on their precise effects on complex ecosystems. As a result, no legislative regulations exist to control MP concentrations in wastewater. Although these substances are typically present in trace amounts in the environment, some have the potential to significantly disrupt natural biological processes. However, as discussed in the introduction, recent EU Commission strategies highlight the urgent need for quaternary treatment in WWTPs to effectively remove MPs. While primary, secondary, and tertiary treatments address conventional pollutants, additional treatment steps are necessary to manage persistent organic contaminants. This regulatory push underscores the need for innovative treatment solutions capable of removing a broader spectrum of pollutants [3; 9; 12].

One concerning group of MPs is endocrine disruptors, which are chemicals capable of interfering with hormonal systems in organisms. Studies have shown their negative effects on fish, including reproductive issues and even physiological and anatomical changes. Beyond their long-term impact on ecosystems, the continuous discharge of MPs may also affect the quality of raw water intended for human consumption [12].

A common type of micropollutant found in wastewater is pharmaceutical residues. These include remnants of antibiotics, contraceptives, antidepressants, painkillers, and even illegal drugs. Pharmaceutical compounds primarily enter wastewater through human excretion via household sewage, as well as from hospital effluents and agricultural activities involving livestock [9; 13].

The release of pharmaceuticals and their metabolites into water bodies has been observed worldwide. In many cases, pharmaceutical residues have been detected in their original form, even after wastewater has undergone all stages of treatment at a WWTP. Despite extensive research on the environmental fate of pharmaceuticals, knowledge of their long-term effects remains limited. This highlights the urgent need for the development of more effective methods for removing MPs from wastewater [13].

The fate of MPs in the environment depends on their physical and chemical properties, such as solubility and the octanol-water partition coefficient. Additionally, MPs can interact unpredictably with one another, potentially leading to indirect environmental effects. While their sources and receptors are defined, the pathways that connect them remain largely unknown. This is due to limited data on the specific physical and chemical characteristics of MPs, as well as the complexity of their behaviour in environmental systems, particularly at trace concentrations [9; 13].

As mentioned earlier, conventional wastewater treatment techniques primarily focus on reducing BOD<sub>5</sub>, suspended solids, N<sub>total</sub>, and P<sub>total</sub>. However, these methods are ineffective at removing complex, non-biodegradable compounds, which consequently enter the environment and may cause harm. To eliminate these substances, more advanced and efficient treatment processes are required, such as AOPs. These methods, which involve the *in situ* generation of highly reactive chemical oxidants like hydroxyl radicals ( $\bullet\text{OH}$ ), have recently emerged as a crucial class of treatment technologies [14].

## 2.2 Theoretical background on AOPs

AOPs offer a promising solution for treating contaminated wastewater containing persistent, nonbiodegradable organic pollutants that resist degradation by conventional treatment methods. AOPs are also used for disinfecting and purifying drinking water. These processes are based on the *in situ* generation of highly reactive oxidizing agents, called reactive oxygen species (ROS), such as  $\bullet\text{OH}$  or other oxidative species. These species accelerate the breakdown and elimination of various organic contaminants from wastewater [14; 4].

The concept of AOPs was introduced in 1987 when they were defined as water treatment methods that operate under room temperature and normal pressure conditions with the production of  $\bullet\text{OH}$  in high enough concentrations to effectively purify water. The Fenton method is the earliest and widely used chemical AOP. It involves the use of Fenton's reagent, a combination of a soluble iron(II) salt ( $\text{Fe}^{2+}$ ) and hydrogen peroxide ( $\text{H}_2\text{O}_2$ ), to break down and eliminate persistent organic pollutants (POPs). The oxidation efficiency and practicality of this method can be significantly enhanced by exposing the treated water sample to ultraviolet (UV) light (photo-Fenton method) or sunlight (solar photo-Fenton method) [15; 5].

Additionally, other photochemical techniques, such as heterogeneous photocatalysis using titanium dioxide ( $\text{TiO}_2$ ) suspensions, as well as ozonolysis ( $\text{O}_3 + \text{UV}$  irradiation), have been explored. Another notable advancement involves integrating the Fenton process with electrochemical reactions, leading to the development of various electrochemical advanced oxidation processes (EAOPs), which have gained attention in recent years. These methods are considered emerging and environmentally friendly, as they utilize electrons as a clean reagent, significantly reducing or eliminating the need for chemical additives [5].

ROS are among the most powerful oxidants in water treatment, capable of reacting with nearly any compound present in the water matrix. Due to their non-selective nature, ROS rapidly break down pollutants and ultimately fragment them into smaller inorganic molecules such as  $\text{H}_2\text{O}$  or  $\text{CO}_2$ . Their production usually involves primary oxidants, such as ozone ( $\text{O}_3$ ),  $\text{H}_2\text{O}_2$ , or oxygen ( $\text{O}_2$ ), energy sources (such as UV light), or catalysts (such as  $\text{TiO}_2$ ). Optimized combinations of these reagents, applied in controlled dosages and sequences, ensure maximum ROS yield. When properly fine-tuned, AOPs can reduce contaminant concentrations from hundreds of ppm to below 5 ppb, significantly lowering chemical oxygen demand (COD) and TOC levels [15; 16].

ROS consists of oxygen-based free radicals, including superoxide ( $\text{O}_2^{\cdot-}$ ),  $\cdot\text{OH}$ , and peroxy radical ( $\text{ROO}\cdot$ ), as well as non-radical molecules like  $\text{H}_2\text{O}_2$ . Although non-radicals are not free radicals themselves, they act as oxidizing agents or can readily convert into radical forms. ROS are oxygen-containing molecules with one or more unpaired electrons in their atomic or molecular orbitals. For instance, when  $\text{O}_2$  gains an extra electron, it forms  $\text{O}_2^{\cdot-}$ , which is the primary type of ROS. They interact with nearby molecules and have extremely short lifespans, usually lasting from nanoseconds to milliseconds [17]. Reduction of oxygen into ROS and their possible byproducts can be observed in Figure 2. MPO stands for myeloperoxidase, SOD for superoxide dismutase and LH are lipids.

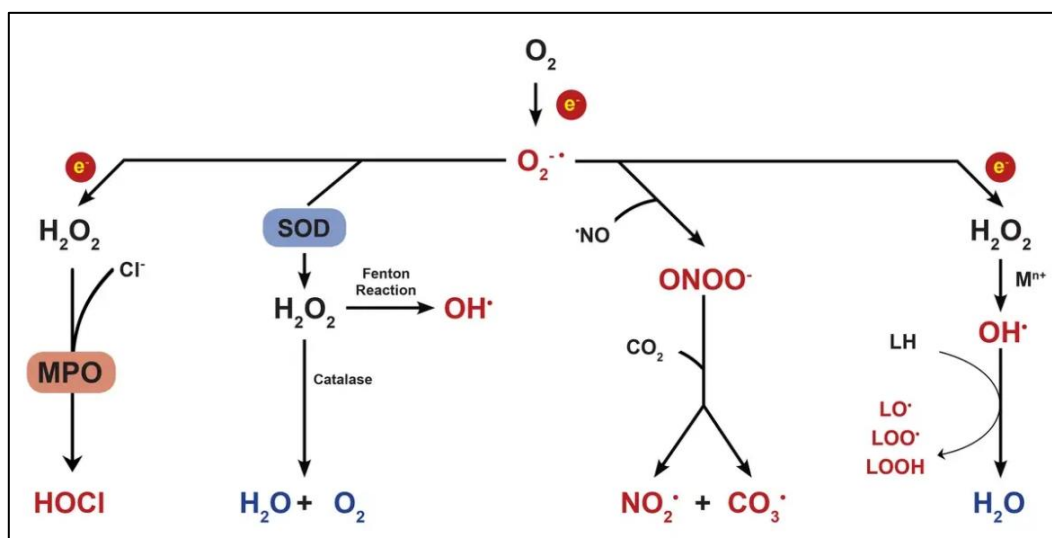


Figure 2 Reduction of oxygen into ROS [18]

The chemical processes in AOPs can be categorized into three main stages (see Figure 3). The first (1) involves the generation of ROS, with the specific production method varying depending on the AOP technique used. In the second stage (2), these radicals react with target pollutants, breaking them down into smaller fragments. Studies have provided insights into this step, revealing that ROS, as highly reactive electrophiles, primarily initiate degradation through hydrogen abstraction or addition reactions. The type of reaction depends on the nature of the organic compound. ROS can abstract a hydrogen atom to form water when reacting with alkanes or alcohols (for example methanol), while in the case of aromatic compounds (such as benzene), it tends to add directly to the molecule. However, the final stage (3), where intermediate compounds undergo further breakdown, remains less understood. Despite this, it is known that continuous reactions with  $\bullet\text{OH}$  ultimately lead to complete mineralization, transforming contaminants into harmless substances like  $\text{H}_2\text{O}$  or  $\text{CO}_2$  [19].

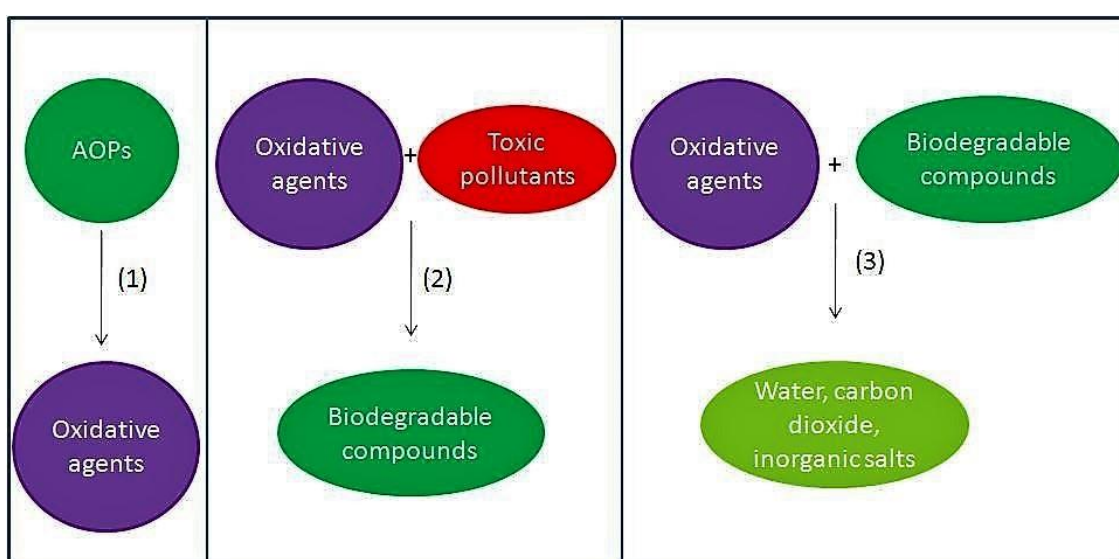


Figure 3 Main steps involved in an AOPs treatment [20]

AOPs are generally divided into chemical, photochemical, and electrochemical methods. The first indication of chemical AOPs appeared with the introduction of the Fenton reagent, a combination of  $\text{H}_2\text{O}_2$  and ferrous salt, which was initially applied for the decomposition of tartaric acid. Over the 20th century, the Fenton process underwent significant advancements and became widely used in water and soil treatment, leading to numerous review studies on its applications [5; 21; 22].

Recent research has confirmed that the Fenton reaction is driven by the generation of  $\bullet\text{OH}$ , which aligns with its classical reaction mechanism. This insight has further established its effectiveness in the degradation and removal of various organic pollutants.

For the Fenton process to function efficiently, the pH of the contaminated water must be maintained within an optimal range of 2.8 to 3.0. Moreover, its overall effectiveness is influenced by several key factors, such as temperature,  $\text{H}_2\text{O}_2$  concentration and catalyst concentration. These elements regulate both the regeneration of  $\text{Fe}^{2+}$  from iron(III) ( $\text{Fe}^{3+}$ ), which forms during the reaction, and the oxidation rate of organic pollutants by the generated  $\bullet\text{OH}$  [5].

Peroxonation is another chemical AOP that utilizes a combination of O<sub>3</sub> and H<sub>2</sub>O<sub>2</sub> to generate reactive oxidative radicals. This method is considered more efficient than ozonation alone because H<sub>2</sub>O<sub>2</sub> enhances the breakdown of O<sub>3</sub> in water, resulting in a greater production of highly reactive •OH.

The O<sub>3</sub>/H<sub>2</sub>O<sub>2</sub> oxidation system can be implemented in a WWTP setup, positioned between sand filtration and activated carbon filtration, within a reactor through which wastewater flows. The main objective of peroxonation in wastewater treatment is to effectively lower micropollutant concentrations before activated carbon filtration, thereby prolonging the operational lifespan of the activated carbon filter [6].

Photochemical AOPs are considered more effective than chemical processes. As a result, UV radiation has been combined with powerful oxidants like O<sub>3</sub> and H<sub>2</sub>O<sub>2</sub>, and in some instances, catalysis with Fe<sup>3+</sup> or TiO<sub>2</sub>. These photochemical processes can effectively degrade or eliminate pollutants through three main mechanisms: UV radiation-induced photodecomposition, excitation and degradation of pollutant molecules, direct oxidation by O<sub>3</sub> and H<sub>2</sub>O<sub>2</sub>, and photocatalytic oxidation (using Fe<sup>3+</sup> or TiO<sub>2</sub>), which triggers the formation of •OH [5; 6].

Among these, VIS light photocatalysis has gained significant attention in recent years as an environmentally friendly alternative. One of its key advantages is the ability of photocatalysts to apply sunlight, which is an abundant, clean, renewable, and cost-effective energy source. While metal-based photocatalysts have been extensively studied, increasing interest is being directed toward metal-free organic dyes as greener alternatives for wastewater treatment. In this context, riboflavin (RF), a naturally occurring compound found in fruits, vegetables, and microorganisms, has emerged as a promising photocatalyst. This dye efficiently absorbs VIS light, generating excited states and ROS, which play a crucial role in the photocatalytic degradation of contaminants [4].

Electrochemical oxidation as a part of EAOPs offers an alternative method for wastewater treatment that eliminates the need for additional chemical reagents. This makes it especially attractive from an environmental perspective, as it provides a clean and efficient means of generating •OH *in situ*, which are highly effective at breaking down large quantities of toxic substances and POPs [5].

These •OH can be produced electrochemically either directly through the AO process or indirectly via the *in situ* generation of Fenton's reagent through an electrocatalytic approach. In direct electrochemical oxidation, pollutants are oxidized through charge transfer reactions after being adsorbed onto the anode surface. Conversely, indirect oxidation relies on redox mediators present in the solution to facilitate pollutant degradation, thereby preventing direct electron transfer between the electrode and contaminants and reducing the risk of electrode fouling [16].

EAOPs have emerged over the past decade, gaining considerable attention for their safety, environmental compatibility, versatility and high efficiency. A key advantage of electrochemical processes is their ability to generate and control •OH *in situ*, without the need for additional chemical reagents or large quantities of catalyst in the medium. This makes it possible to safely discharge treated wastewater directly into natural water sources [5].

In summary, AOPs represent a powerful and versatile approach for treating wastewater contaminated with POPs that are resistant to conventional methods. As environmental concerns and the need for sustainable wastewater treatment solutions continue to grow, AOPs offer an environmentally friendly, efficient, and adaptable methods of addressing complex wastewater contamination, with promising potential for future progress in the field.

### 2.3 Electrochemical systems

In electrochemical systems, our focus is on the processes and factors influencing the movement of charge across the boundary between different chemical phases, such as between an electronic conductor like an electrode and an ionic conductor - an electrolyte. This boundary is called electrode | electrolyte interface. Most often, current flows through this interface after an application of an electric potential [23].

The electrochemical experiments are performed in electroanalytical (electrochemical) cell. Electrochemical cells are generally described as two electrodes separated by one electrolyte phase, which contain analyte of interest. One of the electrodes, known as the working electrode, is that where the target analyte undergoes an electrochemical reaction on its surface. The second electrode, known as the reference electrode, offers a stable and consistent potential, unaffected by the sample composition, against which the potential of the working electrode is measured. In contemporary electrochemical experiments, a third electrode, known as the auxiliary electrode, is used. This electrode is made from an inert conductive material, such as platinum wire. In a three-electrode system, the electric current flows between the working electrode and the auxiliary electrode. There may also be a bubbler tube in the system that serves to supply a gas, such as argon (Ar) or nitrogen (N<sub>2</sub>) that removes dissolved oxygen from the electrolyte or a stir bar [24; 25]. Figure 4 shows an electrochemical cell with a system of three electrodes.

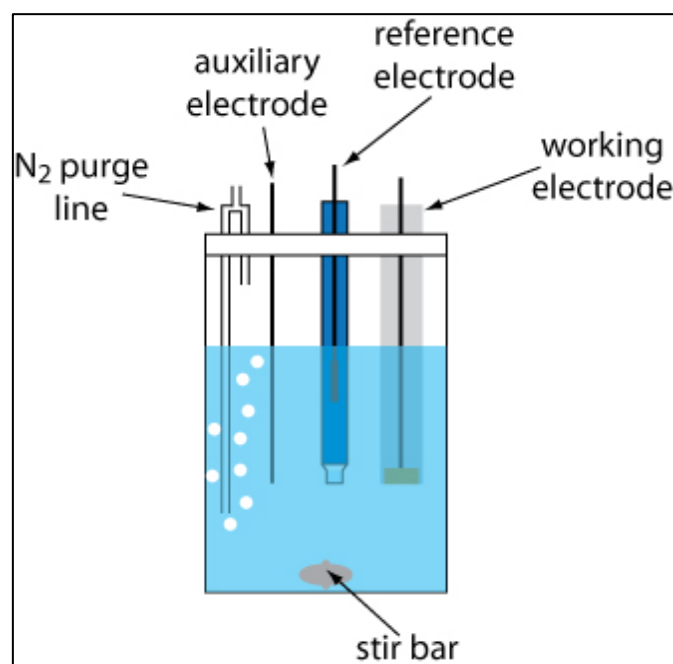


Figure 4 Electrochemical three-electrode cell [26]

Common materials for working electrodes include solid metals like platinum and gold, liquid metals such as mercury or amalgams, and carbon in the form of graphite. Electrode materials can be modified to improve the electrode properties. In the electrolyte phase, charge is transferred through the movement of ions. The most used electrolytes are liquid solutions containing ionic species, such as  $H^+$ ,  $Na^+$ , and  $Cl^-$ , dissolved in  $H_2O$  or a nonaqueous solvent. For an electrochemical cell to be effective, the electrolyte system must be adequately conductive for the intended experiment [23; 24].

Design of the specific electrochemical cell and the material of the electrodes are chosen based on the requirements of the experiment and the characteristics of the sample. The different designs vary in terms of size, temperature control capabilities, stirring needs, shape, and the number of cell compartments. Glass is often used as the cell material because it is inexpensive, transparent, chemically inert, and impermeable. Other potential materials for cell construction include Teflon and quartz. The cell cover can be made from any appropriate material that is inert to the sample [25].

### 2.3.1 Working electrodes

The material of the working electrode plays a critical role in voltammetry, influencing both signal quality and response consistency. Its selection primarily depends on the redox behaviour of the analyte and the background current within the required potential range. Other factors to consider include the potential window, electrical conductivity, surface consistency, mechanical properties, cost, availability, and toxicity. Common working electrode materials used in electroanalysis include mercury, carbon, and noble metals such as platinum and gold [25].

Mercury is often used material for working electrode mainly due to its high reproducibility and unique analytical performance. Mercury based electrodes have been widely used in polarography and are recognized as an effective method for identifying both organic and inorganic analytes. High hydrogen overvoltage is also one of the characteristics of mercury electrodes. During this, cathodic potential window is greatly extended in comparison to solid electrode materials. The disadvantage of mercury in electrodes is its toxicity and mechanical instability [25; 27].

Platinum-based working electrodes have been used for the advantageous properties of platinum as a material, such as its softness, malleability and ductility. Platinum is highly resistant to corrosion and remains nonreactive. These electrodes come in various forms, with the most common types being wires of different diameters and foils of varying thicknesses. A limitation of platinum-based electrodes is their low hydrogen overvoltage, which restricts the cathodic potential range of these electrodes [27].

Another type of working electrode material is gold used for its purity, high conductivity corrosion resistance and the inert behaviour in the presence of almost all reagents. Gold electrodes function similarly to platinum electrodes, but their performance in the positive potential range is significantly limited due to surface oxidation [27].

Carbon-based solid electrodes are widely used in electroanalysis due to their broad potential window, low background current, versatile surface chemistry, affordability, chemical stability,

and suitability for various sensing and detection applications. However, electron transfer rates at carbon surfaces are generally slower compared to metal electrodes. The type of carbon and the pretreatment method significantly impact the analytical performance of the electrode. Common carbon electrode materials include glassy carbon (GC), carbon paste, pyrolytic graphite, carbon fibre, screen-printed carbon strips, carbon films, and other carbon composites [25].

GC electrodes are very often used due to their outstanding mechanical and electrical properties, broad potential window, chemical resistance to solvents, and relatively consistent performance. The material is produced through a carefully controlled heating process of a pre-shaped polymeric phenol-formaldehyde resin in an inert atmosphere. This process is called carbonization. Temperatures during this process reach up to 1200 °C, also this process is slow to ensure all the oxygen, nitrogen and hydrogen is eliminated. GC's structure consists of thin, intertwined ribbons of cross-linked, graphite-like layers. Due to its high density and small pore size, no impregnation process is needed. However, surface pretreatment is commonly used to produce active, consistent GC electrodes and improve their analytical performance. Additional activation methods, including electrochemical, chemical, thermal, or laser treatments, have been employed to further improve performance [25].

Carbon paste electrodes (CPEs), made from graphite powder mixed with nonconductive, water-immiscible organic binders (pasting liquids such as silicone oil), provide a low-cost option with an easily renewable and modifiable surface, along with minimal background current interference. Surface of the electrode can be modified when the solid of the interest is added in to the paste, then the electrode is called modified CPE. CPE was developed to measure the redox potentials of slightly soluble organic compounds, which would otherwise require the use of polarography in organic solvents, resulting in higher sample consumption. It has been noted that these insoluble materials do not need to dissolve before undergoing electrochemical reactions in case of using CPEs. Clays and zeolites are often used solids for modifying CPEs with substantially enhance their specificity or sensitivity in the quantitative analysis of a dissolved target compound. One of the disadvantages of CPEs is their limited mechanical stability [25; 28].

Currently, there is a great interest in the use of pencil graphite electrodes (PGEs) as working electrodes. Pencil graphite (PG) is a readily available, low-cost carbon-based material, making it suitable for use as single-use, disposable electrodes. The compact, highly conductive pencil leads consist of multiple graphene layers intertwined with graphite chunk particles, despite the presence of non-conductive clay components [29; 30].

There are generally two main types of pencil leads available: thicker wood case pencil leads and thinner leads for mechanical pencils. The second group of pencils, which diameter with 0.5 mm is being the most common, is more resilient and elastic compared to wood case pencil leads. The production of mechanical pencils includes high-temperature carbonization of a mixture of graphite and natural high polymers such as cellulose in an oxygen-free environment. In most analyses, the surface of pencil leads is first modified by electrocatalytic layers [29].

PGEs are commonly used as voltammetric sensors in analytical chemistry for a range of electrochemical analyses. They play a crucial role in detecting various environmental pollutants, such as pesticides, pharmaceuticals, food adulterants, metal ions, and antioxidants [30].

During last two decades, boron-doped diamond (BDD) working electrodes have become widely used for their unique electrochemical properties. This type of electrode was firstly used for purification and wastewater treatment, however recently there are also applied to environmental monitoring and biomedical measurements. In the scope of wastewater treatment, BDD electrodes have been used for decomposition of organic compounds due to their ability to produce  $\bullet\text{OH}$  through anodic polarization in neutral or basic environments.

Pure diamond has high electrical resistivity; therefore, a dopant must be incorporated into its structure. As a dopant, boron is the most used for its low charge carrier activation energy. Boron-doped electrode is typically made by chemical vapor deposition of a methane ( $\text{CH}_4$ )/ hydrogen ( $\text{H}_2$ )/ diboran ( $\text{B}_2\text{H}_6$ ) mixture onto a carrier like silicon, tungsten, titanium, niobium, platinum, or molybdenum [31; 32].

Examples of working electrode materials can be observed in Figure 5.

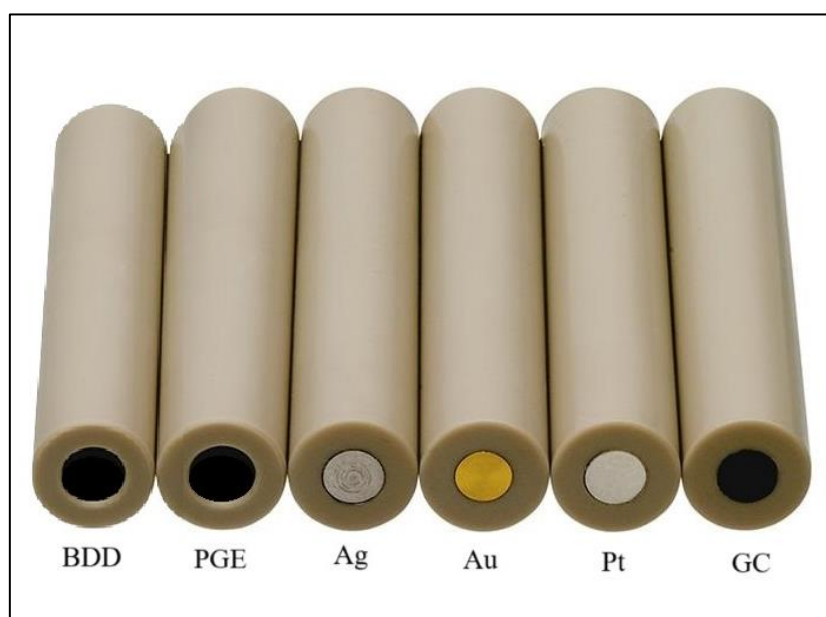


*Figure 5 Examples of working electrodes, adapted from [33]*

### 2.3.2 Reference electrodes

Reference electrodes provide a potential value against which other potentials are measured as differences, since potentials can only be recorded relative to a chosen reference value. A reliable reference electrode needs to meet several requirements regarding its potential. Its potential must be stable with time and temperature and cannot be modified by small disturbances of the systems, such as small current passage [34].

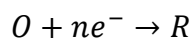
### 2.3.3 Auxiliary electrodes

The auxiliary electrode serves as a means of providing an input potential to the working electrode. This connects the circuit and allows the charge to pass through. The material of these electrodes must therefore be inert, such as carbon or platinum. Also, the area of the electrode surface must be much larger than the area of the working electrode to ensure that no current limitation arise [35].

### 2.4 Electrode | electrolyte interface

When an electric potential is applied and current flows, electrochemical reactions at the electrode | electrolyte interface are taking place. These heterogenic electrochemical reactions involve charge transfer between the electrode and electrolyte [23; 34].

The electrode can function solely as a source (for reduction) or a sink (for oxidation) of electrons, which are transferred to or from species in the solution. The process is described by the equation below, where O and R represent the oxidized and reduced species, respectively.



In the case of reduction, the electrons supplied by the electrode must possess a minimum amount of energy for the transfer to take place, which is associated with a sufficiently negative potential (measured in volts). For oxidation, the lowest unoccupied energy level in the electrode must have a maximum energy to accept electrons from species in the solution, corresponding to a sufficiently positive potential (measured in volts).

In the region near the electrode, the charge distribution differs from that in the bulk solution, causing the energy levels of both the reacting species and the electrode to deviate from those in the bulk phases. For electron transfer to occur, soluble species may need to undergo conformational adjustments. These effects should be corrected for in the study of electrode process kinetics. A thinner interfacial region simplifies this correction, which can be achieved by adding a large concentration of inert electrolyte to the solution [34].

An important aspect of this interfacial region is the formation of the electrical double layer, which plays a key role in charge distribution and influences the behaviour of the system near the electrode. The electrical double layer refers to the arrangement of charged particles and/or oriented dipoles present at any material interface. In electrochemical systems, this layer forms as ionic regions in the solution to balance the excess charge present on the electrode.

A positively charged electrode attracts a layer of negative ions, and a negatively charged electrode attracts positive ions. To maintain electrical neutrality at the interface, the charge on the electrode ( $q_e$ ) and the charge from the nearby ions in the solution ( $q_s$ ) must balance each other, meaning  $q_e + q_s = 0$ . As a result, this counter layer is made up of ions with a charge opposite to that of the electrode [25]. In Figure 6 we can see the ion distribution at an electrode surface.

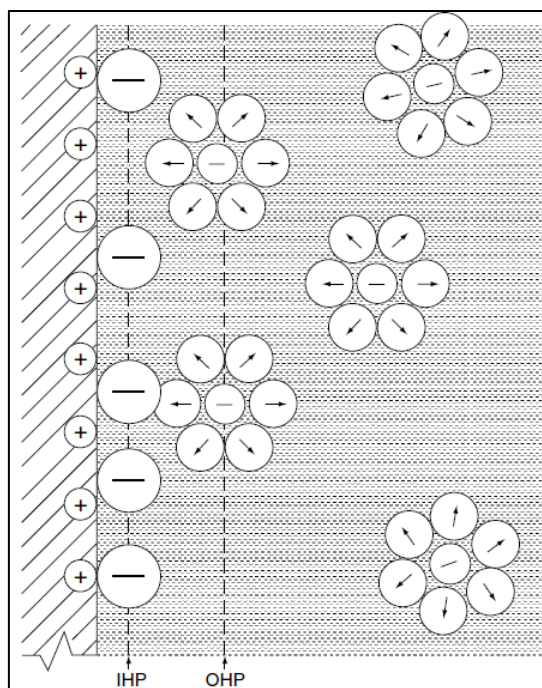


Figure 6 Distribution of ions in electrical double layer [25]

The layer closest to the electrode, called the inner Helmholtz plane (IHP), consists of solvent molecules. This layer is defined by the positions of these specifically adsorbed ions. Beyond this is the outer Helmholtz plane (OHP), an imaginary plane that passes through the centre of solvated ions at their closest approach to the electrode surface. These solvated ions are non-specifically adsorbed and attracted by long-range Coulombic forces. Both IHP and OHP together form the compact layer, a tightly bound structure of charges that remains attached to the electrode even if it is removed from the solution. The Helmholtz model, however, does not account for the thermal motion of ions, which can loosen them from the compact layer. Beyond this compact layer is the diffuse layer (or Gouy layer), a three-dimensional region of dispersed ions that extends from the OHP into the bulk solution [23; 25].

Two basic types of processes can take place at electrodes. These reactions follow Faraday's law, which states that the amount of chemical change is directly proportional to the electrical charge passed through the system. One type, as mentioned above, involves reactions where charges, such as electrons, are exchanged across the metal-solution interface, leading to oxidation or reduction. Consequently, these are known as faradaic processes. In the second case, in certain conditions, an electrode-solution interface may exhibit a range of potentials where no charge-transfer reactions take place, as these reactions are either thermodynamically or kinetically unfavourable. However, processes like adsorption and desorption can still occur, and the structure of the electrode-solution interface may vary with changes in potential or the composition of the solution. These are known as nonfaradaic processes [23]. The processes taking place on the electrode surface are illustrated in Figure 7.

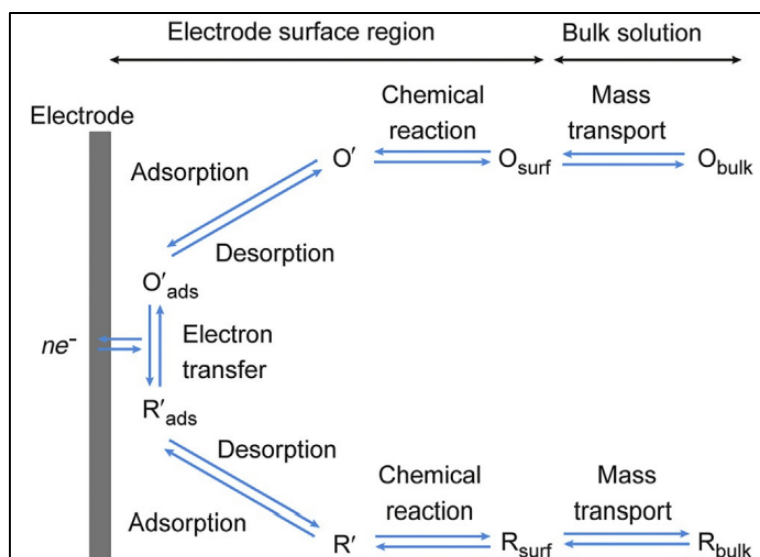
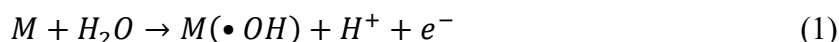


Figure 7 Processes at the electrode surface [36]

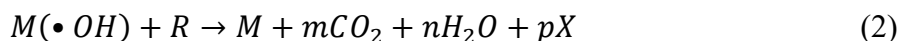
## 2.5 Principles of AO

AO, a type of EAOP, offers a direct and environmentally friendly method for electrochemically producing  $\bullet\text{OH}$  radicals without the need for additional chemical reagents, since electrons serve as the reactant. These  $\bullet\text{OH}$  are generated directly at the anode surface through the oxidation of  $\text{H}_2\text{O}$ , facilitated by anodes with a high oxygen evolution overvoltage [5].

The catalytic mechanism of AO involves the generation of  $\bullet\text{OH}$  and their role in breaking down organic pollutants, see equation (1). In the first step,  $\text{H}_2\text{O}$  is oxidized at the anode surface (M), producing  $\bullet\text{OH}$  ( $\text{M}\bullet\text{OH}$ ) that remains adsorbed on the electrode while releasing protons ( $\text{H}^+$ ) and electrons ( $\text{e}^-$ ) into the solution. While at the cathode, hydrogen gas is produced, which does not participate in pollutant oxidation. As a result, the electrochemical wastewater treatment process primarily targets AO [5; 37].



Once produced, these highly reactive  $\bullet\text{OH}$  play an important role in breaking down pollutants. The radicals attack organic pollutants (R), decomposing them into  $\text{CO}_2$ ,  $\text{H}_2\text{O}$ , and inorganic byproducts (X), such as chloride ions from chlorine-containing compounds, see equation (2).



The anode itself acts as a catalyst, enabling continuous radical formation and pollutant degradation without being consumed. This mechanism demonstrates the efficiency of AO as a clean and sustainable method for wastewater treatment [5].

It has been demonstrated that electrode materials are crucial in electrochemical oxidation, as they impact the efficiency of oxidation, degradation processes, and the mechanisms of the reactions. The BDD anode has emerged as a highly promising material for the electrochemical

treatment of wastewater containing organic pollutants. One of its key advantages is its significantly higher oxygen evolution overvoltage than conventional materials like platinum, lead dioxide or iridium dioxide. This high overvoltage allows the BDD anode to generate larger amounts of highly reactive  $\bullet\text{OH}$  adsorbed on its surface, rather than the production of unwanted byproducts like oxygen gas, making it more effective at breaking down pollutants than other anode materials [5; 37].

In addition to the electrode materials, the efficiency of electrochemical oxidation is closely linked to the supporting medium. When electrolytes like sulphate or phosphate are used, they can lead to the formation of less powerful oxidizing agents, such as peroxydisulfate and peroxodiphosphate, during the AO process. This underlines the importance of carefully selecting the appropriate electrolytic medium to maximize the effectiveness of AO for wastewater treatment [37].

## 2.6 Electrochemical methods

One of the most utilized electrochemical methods are voltammetries. All voltammetric techniques share the core feature of applying a potential ( $E$ ) to an electrode and tracking the resulting current ( $I$ ) that flows through the electrochemical cell. Often, the potential is adjusted, or the current is measured over a certain time ( $t$ ). This means that all voltammetric methods can be represented as functions involving  $E$ ,  $I$ , and  $t$ . These methods are considered active techniques, unlike passive methods like potentiometry, since the applied potential actively drives a change in the concentration of electroactive species at the electrode surface by reducing or oxidizing them. When a substance undergoes redox reactions at the working electrode surface at a suitable applied potential, it drives the transport of analyte molecules from the solution, resulting in a measurable current.

Voltammetric techniques are widely used in analytical chemistry for quantifying dissolved inorganic and organic substances. They are also valuable in fields like inorganic, physical, and biological chemistry to study oxidation-reduction processes, adsorption, electron transfer, reaction mechanisms, and properties of solvated species. Additionally, voltammetry is applied to pharmaceutical compound analysis and, when paired with HPLC (High Performance Liquid Chromatography), is effective for analysing complex mixtures [38].

### 2.6.1 Cyclic voltammetry

Cyclic voltammetry (CV) involves linearly sweeping the potential of a stationary working electrode (in an unstirred solution) using a triangular waveform. Depending on the desired information, either single or multiple cycles can be applied. Throughout the sweep, the potentiostat records the current generated by the applied potential. The resulting plot of current versus potential is called a cyclic voltammogram [25].

When a solution containing the oxidized analyte is scanned to negative potentials, it is locally reduced to the reduced analyte at the electrode surface. This reduction generates a measurable current and depletes the oxidized analyte near the electrode. As the potential is scanned in the negative (cathodic) direction from point A to point C (see Figure 8), the concentration of the oxidized analyte near the electrode decreases steadily as it is reduced to the reduced analyte.

At point B, where the peak cathodic current is observed, the current depends on additional oxidized analyte being supplied by diffusion from the bulk solution. The region of solution near the electrode that contains the reduced analyte, known as the diffusion layer, continues to expand throughout the scan. This expansion slows down the transport of the oxidized analyte to the electrode. As a result, when scanning to more negative potentials, the rate of diffusion of the oxidized analyte from the bulk solution to the electrode surface decreases, leading to a drop in current as the scan progresses (from B to C).

Upon reaching the switching potential at point C, the scan direction is reversed, and the potential is scanned in the positive (anodic) direction. While the concentration of the oxidized analyte at the electrode surface has decreased, the concentration of the reduced analyte has increased. As the applied potential shifts more positive, the reduced analyte present at the electrode surface is oxidized back to the oxidized form. The separation between the two peaks arises from the diffusion of the analyte toward and away from the electrode [39].

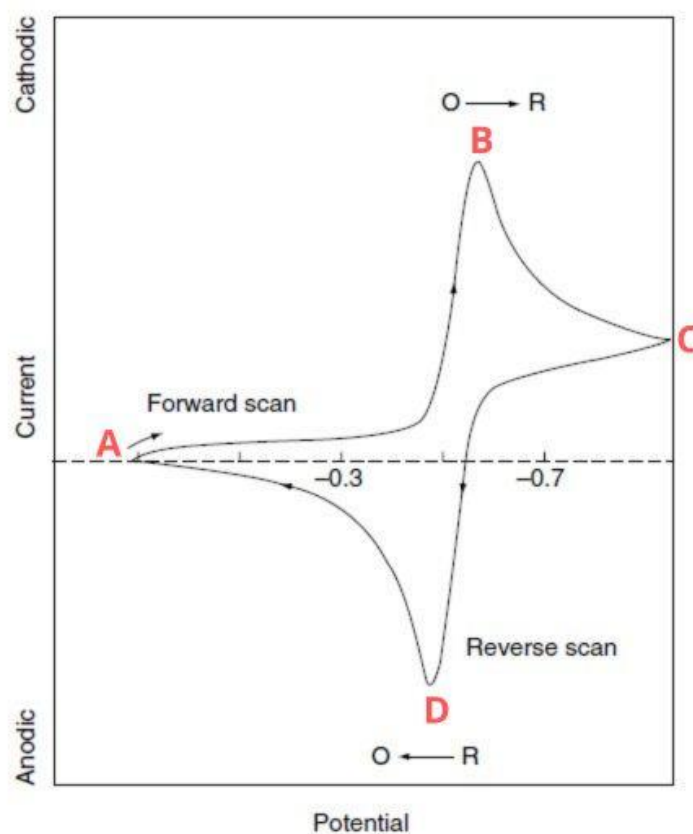


Figure 8 Cyclic voltammogram, adapted from [25]

A reversible electrochemical reaction is one that proceeds so rapidly that it continuously re-establishes equilibrium, even as conditions, like applied potential, change. This allows the concentrations of reactants and products at the electrode surface to adjust in a way that maintains the equilibrium ratio predicted by the Nernst equation (3). It relates the cell potential ( $E$ ) to the standard potential of a species ( $E^0$ ) and the relative activities of the oxidized and reduced analyte in the system at equilibrium. In the equation,  $F$  is Faraday's constant

(96,485 C/mol),  $R$  is the universal gas constant ( $8.3144 \text{ J mol}^{-1}\text{K}^{-1}$ ),  $n$  is the number of electrons transferred, and  $T$  is the absolute temperature (K). The Nernst equation is a powerful tool for predicting how a system will respond to changes in analyte concentration or electrode potential [38; 39].

$$E = E^0 + \frac{RT}{nF} \ln \frac{[Ox]}{[Red]} \quad (3)$$

### 2.6.2 Square wave voltammetry

Square wave voltammetry (SWV) is one of the pulse voltammetric techniques, which are designed to enhance the sensitivity of electrochemical measurements, enabling the detection of very low concentrations, down to  $10^{-8}$  M. By maximizing the ratio between faradaic (reaction-based) current and non-faradaic (background) current, these techniques allow to more clearly identify and quantify the analyte's signal, even in the presence of noise. These methods involve applying a series of rapid potential pulses to the working electrode, each lasting about several tens of milliseconds. The resulting charging (nonfaradaic) current fades quickly, leaving primarily the faradaic current to be measured, allowing for enhanced discrimination against background signals [25].

SWV is a high-sensitivity technique that applies a distinctive waveform, consisting of a symmetrical square wave overlaid on a gradually increasing baseline voltage (called the staircase potential), to the working electrode. During each cycle of the square wave, two current measurements are taken: one at the end of the forward pulse (at  $t_1$ ) and another at the end of the reverse pulse (at  $t_2$ ). Because of the large amplitude of the square wave modulation, the reverse pulses initiate the reverse reaction of the product formed by the forward pulse. During each potential cycle, the electrode reaction alternates between anodic (oxidation) and cathodic (reduction) processes, offering valuable information about the underlying electrode mechanism [25; 40].

The difference between two measurements is then plotted against the staircase potential, providing a clear and detailed profile of the electrochemical reaction [25]. Below we can see Figure 9 showing the basic principle of the SWV technique. It illustrates the square wave amplitude  $E_{sw}$ , step height  $\Delta E_{sw}$ , square wave period  $\tau$ , delay time  $T_d$  and the times for current measurements 1 and 2.

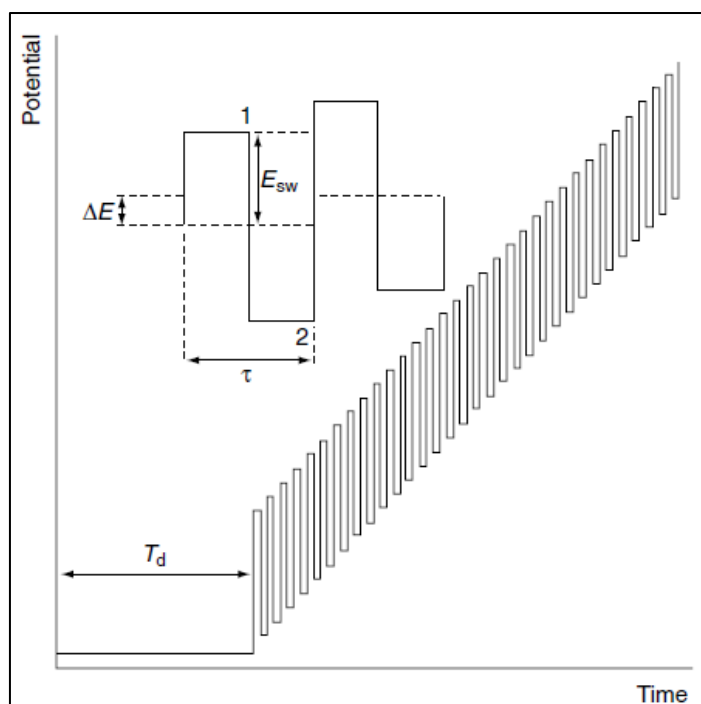


Figure 9 Principle of the SWV [25]

The exceptional analytical sensitivity SWV makes it widely utilized for the quantitative analysis of various substances, including pharmaceuticals, biomolecules, environmental pollutants, antioxidants, and more. In addition to its high sensitivity, SWV is recognized as a rapid electroanalytical method, requiring minimal analysis time. Its sensitivity can be further enhanced when combined with enrichment techniques commonly used in electroanalysis, such as electrolytic or adsorptive accumulation. Over the past decade, SWV has often been adopted as a cost-effective and efficient alternative to more expensive and time-intensive methods, such as chromatography, for analysing inorganic and biologically significant compounds [40].

### 2.6.3 Chronoamperometry

Chronoamperometry is a fundamental electrochemical technique in which a constant potential is applied to an electrode, and the resulting current is recorded as a function of time. Initially, the potential is held at a value where no electrochemical reactions occur, followed by a rapid step to a potential that induces the desired redox reaction, such as oxidation or reduction. This potential step leads to an immediate surge in current due to the rapid consumption of analyte near the electrode surface. Over time, the current diminishes as the local concentration of the reactant decreases, and diffusion becomes the primary mechanism replenishing the electrode surface. Eventually, the current stabilizes to a steady-state value proportional to the analyte concentration [36]. Typical diagram for chronoamperometric methods is shown in Figure 10.

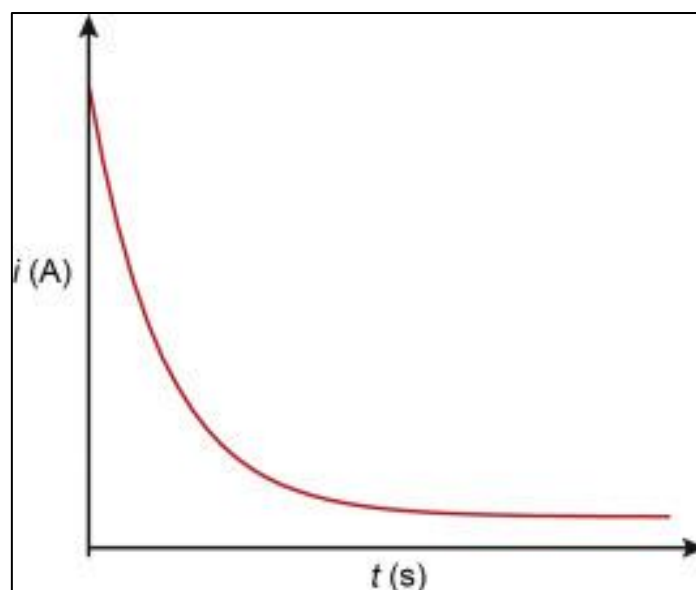


Figure 10 Typical diagram for chronoamperometric methods [36]

Controlled potential (bulk) electrolysis (CPE), also referred to as potentiostatic coulometry, is an application of chronoamperometry. In this technique, a fixed potential is applied to the working electrode while the current is recorded over time. The analyte undergoes oxidation or reduction, transitioning from one oxidation state to another.

As the analyte is progressively depleted, the current diminishes and eventually approaches baseline levels near zero. The potential applied to the working electrode during CPE is chosen based on the specific redox pair that initiates electrocatalytic activity. This potential is typically determined through CV or other voltammetric techniques.

Only catalyst molecules near the electrode surface participate in electrocatalytic turnover, making stirring during CPE essential for consistent delivery of analyte. The stirring rate directly affects the CPE current by driving material convection to the electrode. Inconsistent stirring or poor control over the flow can cause variable currents, complicating comparisons among experiments due to dependencies on stir rate and cell geometry [41].

## 2.7 Photocatalysis as an advanced water treatment method

Photocatalysis, a key component of AOPs, has gained significant attention as an advanced water treatment method due to its ability to harness ultraviolet-visible (UV-VIS) light to generate ROS for pollutant degradation. This environmentally friendly process efficiently converts light energy into chemical energy, enabling the breakdown of organic contaminants in a sustainable manner. It is a highly versatile method for wastewater purification, groundwater disinfection, and the removal of a wide range of pollutants, including heavy metals, pharmaceuticals, chlorinated compounds, pesticides, and dioxins. Unlike conventional oxidation techniques, photocatalysis requires no chemical additives, making it a more energy-efficient and sustainable solution. Additionally, it operates under mild pressure and temperature conditions, and when

heterogeneous photocatalysts are used, their easy separation further enhances the process efficiency [42].

Photocatalysis refers to a process in which chemical reactions are driven by light in the presence of a semiconductor. The material that absorbs light and facilitates these reactions is called a photocatalyst, and all photocatalysts function as semiconductors. Semiconductors can conduct electricity even at room temperature when exposed to light, allowing them to function as photocatalysts. When a photocatalyst absorbs light of a suitable wavelength ( $\lambda$ ) with sufficient energy, photons transfer energy to an electron in the valence band, exciting it to the conduction band. This transition leaves behind a hole ( $h^+$ ) in the valence band. As a result, a photoexcited state is created, generating an electron-hole pair.

The excited electron in the conduction band acts as a reducing agent by transferring its energy to an electron-accepting molecule, facilitating reduction reactions. Meanwhile, the  $h^+$  left in the valence band serves as a powerful oxidizing agent, extracting electrons from donor molecules and driving oxidation reactions. This dual functionality of photocatalysts enables oxidation and reduction processes to occur simultaneously. In Figure 11, we can see the dual functionality of photocatalysts in degrading pesticides as MPs [43].

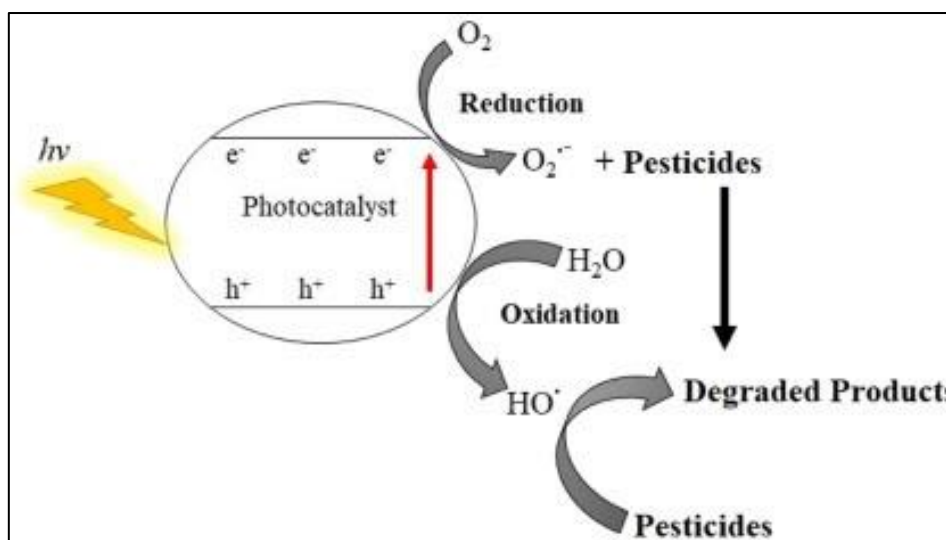


Figure 11 Dual functionality of photocatalysts, adapted from [44]

$TiO_2$  is the most used semiconductor catalyst in photocatalytic processes. It has become the material of choice for heterogeneous photocatalysis in water treatment due to its favourable characteristics.  $TiO_2$  is chemically stable, biologically inert, and relatively inexpensive to produce. It is also highly effective in photocatalysis and has an energy bandgap that aligns well with solar light. Furthermore, the  $h^+$  generated during the photocatalytic process are powerful oxidizing agents, while the electrons produced are strong enough to form  $O_2^{\cdot-}$  from oxygen. The  $TiO_2$  catalyst can be applied either in a dispersed form (powder or aqueous suspension) or as a thin film (in the form of a fixed catalytic layer) [5; 37].

Although extensive research over the past few decades has shown these materials to be highly promising, their practical applications may be limited by certain drawbacks. A limitation of the dispersed form of TiO<sub>2</sub> is the occurrence of dark catalytic sludge, which reduces UV efficiency and photocatalytic performance. TiO<sub>2</sub> films, however, eliminate the need for catalyst separation but require a stable and active layer. The catalyst's quantity and type are influenced by factors like the irradiation source or pollutant properties. Moreover, optimizing the pH of the medium is essential for efficient photocatalysis and should be tailored to the specific pollutant being degraded. However, ongoing research still aim to develop more advanced, durable, and highly efficient photocatalysts based on metal compounds. [5; 45].

In recent years, metal-free photocatalysts have gained significant interest as a promising alternative due to their unique properties and suitability for various photocatalytic reactions. This has led to the development of numerous applications involving metal-free photocatalysts alternatives, such as organic dyes. RF is a naturally occurring dye found in rivers, lakes, and seawater. It exhibits notable structural and optical properties, including a three-ring isoalloxazine core with 7,8-dimethyl substitutions and a ribotyl chain at the N<sub>10</sub> position, as well as distinct absorption peaks around 450 nm and 350-375 nm with high molar absorption coefficients. Due to these properties, RF plays a significant role in the natural photodegradation of environmental pollutants [45; 46].

The potential of RF as a metal-free photocatalyst for water treatment, especially in enhancing the photooxidation of aromatic MPs under sunlight, has been widely researched. More recently, RF and similar flavin derivatives have been utilized as VIS light redox photocatalysts to drive a variety of synthetic reactions. These include processes like the aerobic photooxidation of sulphides and the selective removal of benzylic groups [46].

## 2.8 Molecular Spectroscopy

Molecular spectroscopy is based on the principle that electromagnetic radiation (EMR) interacts with atoms and molecules in specific manners. Its goal is to obtain an optical spectrum, which represents the dependence of the intensity of radiation - whether absorbed, reflected, emitted, or scattered by a substance - on  $\lambda$  [47; 48].

One of the key physical properties of substances is their ability to absorb radiation at specific  $\lambda$ . Rather than being continuous, the absorbed or emitted spectrum is made up of distinct lines that are characteristic of each substance. Each chemical compound has a unique absorption and emission spectrum, ensuring that no two different substances share the same spectral signature [49].

EMR is a form of energy that travels as waves and interacts with matter in discrete ways, playing a crucial role in spectroscopy. It can be described as a sine wave, where  $\lambda$  is the distance between peaks (nm), and frequency ( $\nu$ ) is the number of wave cycles per second, related by the equation (4), where  $c$  is the speed of light in vacuum ( $2.998 \times 10^8 \text{ ms}^{-1}$ ) [47].

$$\nu = \frac{c}{\lambda} \quad (4)$$

Since  $\lambda$  and frequency are inversely related, shorter  $\lambda$  correspond to higher frequencies and higher energy, while longer  $\lambda$  correspond to lower frequencies and lower energy. The electromagnetic spectrum includes various types of radiation, from high-energy gamma rays and X-rays to low-energy radio waves [48]. Illustration of the electromagnetic spectrum can be seen in Figure 12.

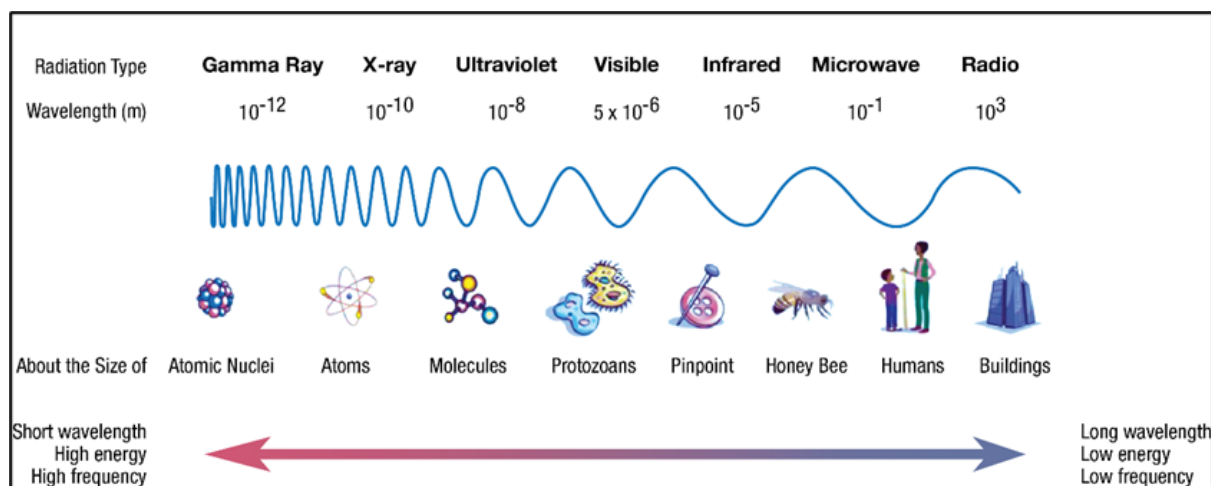


Figure 12 Electromagnetic Spectrum, adapted from [50]

Light exhibits wave-particle duality, meaning it behaves as both a wave and a particle (photon), depending on how they are observed. The energy of a photon is given by equation (5), where  $h$  is Planck's constant ( $6.63 \times 10^{-34}$  Js). This explains why short- $\lambda$  radiation like X-rays is highly energetic, while long- $\lambda$  radiation like radio waves carries little energy.

$$E = \frac{hc}{\lambda} \quad (5)$$

Absorption takes place when a molecule absorbs a photon of a specific energy, promoting an electron from a lower to a higher energy state. The nature of this transition depends on the  $\lambda$  of the radiation: electronic transitions occur in the UV-VIS region, vibrational transitions take place in the infrared (IR) region, and rotational transitions are observed in the microwave region. The energy absorbed must match the energy gap between the two states, leading to characteristic absorption spectra unique to each substance.

### 2.8.1 UV-VIS Spectrophotometry

This technique is one of the most essential and widely applied spectrophotometric techniques for analysing various compounds. It focuses on the absorption of radiation by chemical species in the solution ranging from 180 to 780 nm of electromagnetic spectrum.

In UV-VIS spectroscopy, radiation is absorbed at the electronic energy levels of molecules. However, in solution, the overlap of vibrational and rotational transitions results in a UV-VIS spectrum with minimal detailed structure. Although each molecule has a specific  $\lambda$  at which it absorbs light most strongly, this technique is generally not used for precise molecular

identification. This method can be used to quantify both organic compounds mainly in the UV range and inorganic substances mainly in the VIS range [48; 51].

However, under controlled conditions, the amount of radiation absorbed can be directly related to the concentration of the substance in solution as described by Lambert Beer's law, see equation (6). The equation represents the relationship between light absorption and various factors influencing it. The sample concentration ( $c$ ) is measured in either moles per liter (mol/L) or grams per millilitre (g/mL), while the path length ( $d$ ) represents the distance light travels through the sample (cm). Additionally, the extinction coefficient ( $\epsilon$ ) is a substance-specific constant that quantifies how strongly the sample absorbs light at a given  $\lambda$ , with units of L/(cm·mol) or mL/(cm·g), depending on the chosen concentration unit [51].

$$A = \epsilon \times c \times d \quad (6)$$

As the analyte concentration increases, light absorption rises proportionally, while light transmission decreases exponentially. In the UV-VIS region, radiation absorption is influenced by the electronic structure of the absorbing species, including atoms, molecules, ions, and complexes [48].

UV-VIS spectroscopy is a highly versatile technique with broad applications across various fields. It plays a crucial role in environmental monitoring by identifying and measuring contaminants in air, water, and soil. For instance, in water quality assessment, it helps determine pollutant levels, including oxygen demand, heavy metal ions, nitrate nitrogen, and dissolved organic carbon. Geologists also use this technique to evaluate the effects of mining on water bodies, enabling the detection of trace contaminants and the implementation of protective actions. Additionally, in agriculture, this method is employed to analyse phosphorus levels in animal feed, ensuring regulatory compliance [52; 53].

In the UV-VIS spectroscopy, these substances are analysed using the UV-VIS spectrophotometer. It consists of the following components: light source, monochromator, sample cell, detector and data analysis. The light source in a UV-VIS spectrophotometer generates polychromatic light, covering a broad spectral range to enable accurate measurements. Different lamps are used depending on the  $\lambda$  range required. For UV light, common sources include deuterium, hydrogen, tungsten, mercury, and xenon lamps. For VIS light, tungsten, mercury vapor, and carbon lamps are typically employed [48; 54].

A monochromator is a device that takes in polychromatic light from a lamp and outputs monochromatic light by separating the radiation based on  $\lambda$ . It is involved in dispersing light to isolate specific  $\lambda$  for analysis. The monochromator consists of three components: the entrance slit, which regulates the amount of incoming light; the dispersing device (such as prism or grating), which separates the polychromatic light into individual  $\lambda$ ; and the exit slit, which selects and transmits the desired  $\lambda$  for further measurement.

Cuvettes are designed to hold samples and reference for analysis. They come in various shapes and sizes, differing in path length and light transmission properties based on the required  $\lambda$ . Made from materials such as plastic, glass, or optical-grade quartz, they are selected to ensure minimal absorption within the relevant spectral range. To obtain accurate results, cuvettes must

be cleaned before use, so any residue or contaminants could interfere with spectroscopic measurements.

Detector is an instrument designed to measure the intensity of light transmitted through a sample and to convert the detected light signals into corresponding electrical signals. Photomultiplier tubes are one of the most widely used detectors in spectroscopy. They consist of a photoemissive cathode, multiple dynodes, and an anode. When a photon enters the tube and strikes the cathode, it triggers the release of electrons. These electrons are then accelerated toward the first dynode. Each electron impact on the dynode generates multiple additional electrons, which continue to accelerate through a series of dynodes, amplifying the signal further. Eventually, the accumulated electrons reach the anode, where the signal is collected.

The spectrometer then transmits signals to the recorder, with the intensity of these signals being determined by the analyte's absorption of light at a certain  $\lambda$ . Personal computer then processes the data [48]. Simplified scheme of UV-VIS spectrophotometer can be observed in Figure 13.

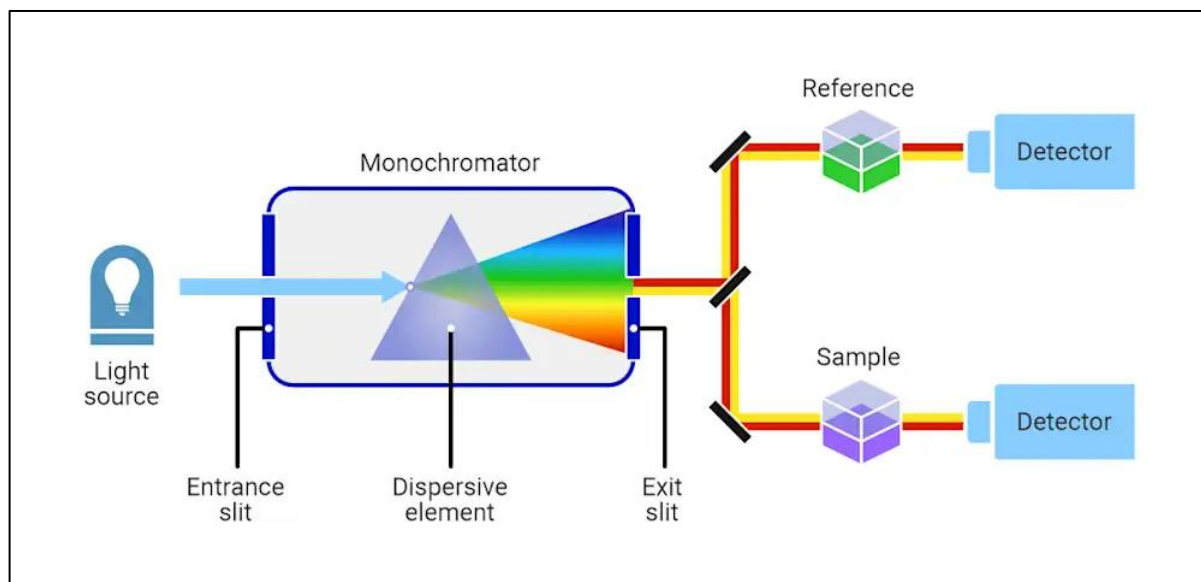


Figure 13 A simplified diagram of the UV-VIS spectrometer [55]

## 2.9 Chemistry of the MB

Methylene blue (MB) is an aromatic heterocyclic compound with the chemical formula  $C_{16}H_{18}N_3SCl$  and is commonly used as a textile dye in various industries. MB is a chemically modified form of phenothiazine. It appears as a dark blue powder that dissolves in water to produce blue solution. In its hydrated state, each molecule of MB is associated with three water molecules. This basic dye has a molecular weight of 319.85 g/mol and absorbs light most strongly at 664 nm. Highly soluble in water, it forms a stable solution at room temperature [56].

MB is generally resistant to degradation through conventional methods like biological treatment or chemical coagulation. However, it can be effectively broken down using EAOPs, which facilitate its complete oxidation. This process results in harmless end products ( $H_2O$  and  $CO_2$ ), minimizing the risk of secondary pollution. See Figure 14 for possible degradation pathways of MB by EAOPs [56; 57].

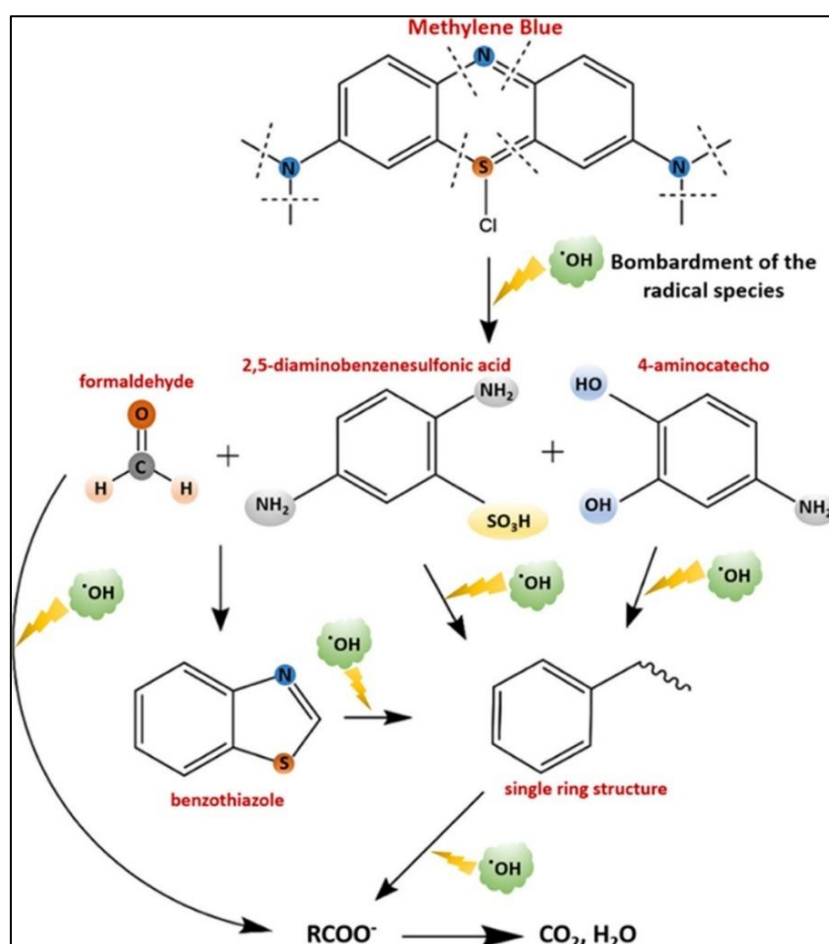


Figure 14 Possible MB degradation pathways using the EAOP process [57]

## 2.10 Chemistry of the Flavin

Flavin catalysis offers an environmentally friendly approach to chemical transformations. In recent years, vitamin  $B_2$ , known as RF and its derivatives (FLs) have emerged as widely used dye-based photoredox catalysts. These compounds serve as powerful redox organocatalysts,

driving various oxidation reactions. RF and FLs exhibit peak absorption in the blue region of the VIS spectrum and possess high molar absorption [58].

A-Na-TEG, full name 1,3-bis(2-(2-(2-methoxyethoxy)ethoxy)ethyl)naphtho[2,3g]pteridine-2,4(1H,3H)-dione, represents a derivative of RF whose chemical formula is  $C_{28}H_{36}N_4O_8$  and molar mass is  $556.61 \text{ g}\cdot\text{mol}^{-1}$ . For RF itself, but also for its FLs, including A-Na-TEG, light-driven production of ROS is assumed, which could then participate in the degradation of organic MPs via photooxidation reactions [46; 59]. Structure of A-Na-TEG is shown in the Figure 15.

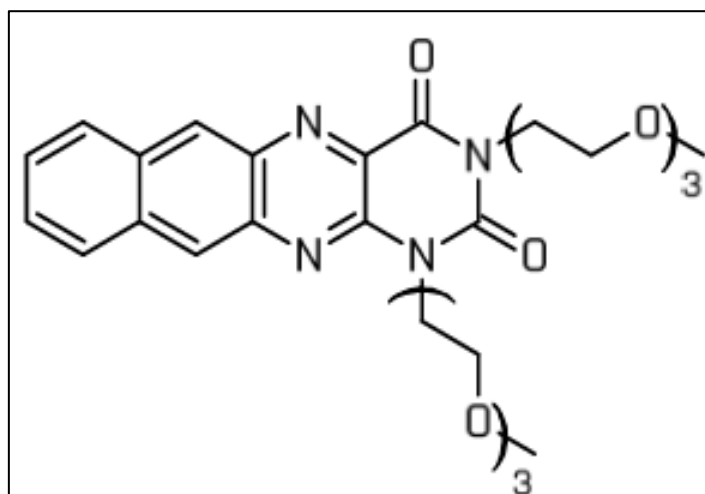


*Figure 15 Structure of A-Na-TEG [59]*

### 3. EXPERIMENTAL PART

#### 3.1 Chemicals

- Methylene Blue hydrate ( $\geq 97.0\%$ ) (Sigma-Aldrich, India)
- Tri-distilled water
- Sodium chloride ( $\text{NaCl} \geq 99.5\%$ ) (Sigma-Aldrich, USA)
- Sodium hydroxide ( $\text{NaOH} \geq 98\%$ ) (Sigma-Aldrich, Sweden)
- Hydrochloric acid ( $\text{HCl} 35\% \text{ p.a.}$ ) (Penta s r.o., Czech Republic)
- Phosphoric acid ( $\text{H}_3\text{PO}_4 85\%$ ) (Fluka, Germany)
- 1,3-bis(2-(2-(2-methoxyethoxy)ethoxy)ethyl)naphtho[2,3-g]pteridine-2,4(1H,3H)-dione (A-Na-TEG) (Faculty of Chemistry BUT, Czech Republic)

#### 3.2 Equipment

- Common laboratory equipment and glass such as flasks, vessels, funnels, spatulas, stand and clamps, Eppendorf tubes
- Analytical balances XS105 (Mettler Toledo, Switzerland)
- Mechanical Pipettes (Eppendorf Research, Germany)
- Test Tube Shaker – Vibrating Relax Top (Heidolph, Germany)
- Personal centrifuge Dr. Spin™ (Genlantis, USA)
- pH Meter Microprocessor pH 213 (Hanna instruments, Italy)
- Spectrophotometer/Fluorometer DS-11 FX+ (DeNovix, USA)
- Magnetic hotplate stirrer MR Hei-Standard (Heidolph, Germany)
- Traceable stopwatch
- Potentiostat/Galvanostat/Impedance analyser PalmSens 3 and 4 (PalmSens BV, Netherlands)
- Spectrophotometer Specord 210 Plus (Analytikjena, Germany)
- Spectrofluorometer (ISS, USA)
- Cable connectors with clips
- Carbon pencils Koh-i-noor Hardtmuth, 4152 HB 60 mm,  $\varnothing 0,5 \text{ mm}$  as Working Electrode
- $\text{Ag}|\text{AgCl}| 3 \text{ M KCl}$  Reference Electrode
- Platinum Auxiliary Electrode
- Quartz Suprasil® cuvettes for UV/VIS (10 mm) (Hellma, Germany)
- Quartz cuvettes (10 mm) (Starna Scientific Ltd., UK)

### 3.3 Preparation of working solutions

For the preparation of the MB working solution, the final concentration was first determined to be 2 mg/mL. A precise mass of 1.98 mg of MB hydrate was weighed using analytical balances. This was then dissolved in 0.99 mL of tri-distilled water. The solution was transferred into a 2 mL Eppendorf tube, vortexed for thorough mixing, and centrifuged. The prepared solution was left to stand for 15 minutes to ensure complete dissolution and stabilization before use. The molar concentration of the MB solution was determined using the absorbance of the solution. The sample was first diluted 1000 times, and the absorbance was then measured at 664 nm using a spectrophotometer. The extinction coefficient was determined to be 74028 L/mol $\times$ cm. Using the Lambert-Beer law equation (6), the concentration of the original solution was calculated to be 8 mM.

The sodium chloride (NaCl) solution was prepared as an electrolyte, with the final concentration set at 0.05 M. A 0.5 mL aliquot of a 5 M NaCl stock solution was pipetted into a 50 mL volumetric flask, and the flask was then filled to the calibration mark with tri-distilled water. The solution was thoroughly mixed and then quantitatively transferred to a glass container with a lid. The pH of the solution was measured and stabilized at 10.2.

For the preparation of the water-soluble flavin solution for the spectrophotometric part of the experiment, 1 mg of flavin A-Na-TEG was dissolved in 1 mL of ultrapure distilled water. The molar concentration of the stock solution was calculated to be 1.8 mM.

### 3.4 Apparatus for electrochemical analysis

Figure 16 shows an electrochemical analysis setup using a three-electrode system. A PGE was employed as the working electrode, while an Ag|AgCl|3M KCl reference electrode and a platinum auxiliary electrode completed the system. The electrodes were securely positioned in an electrode holder and fixed to a laboratory stand using clamps.

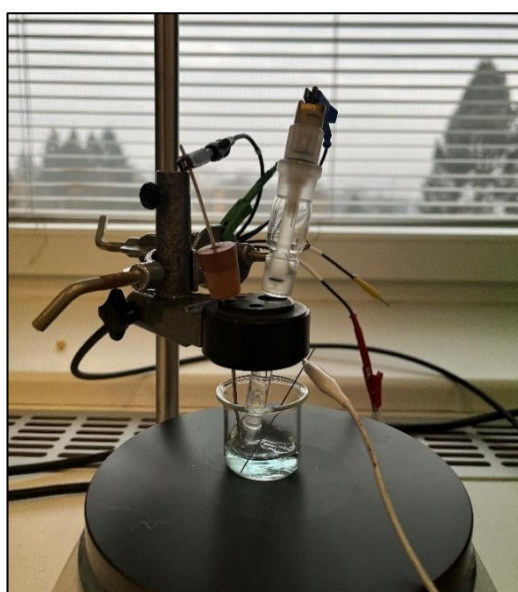
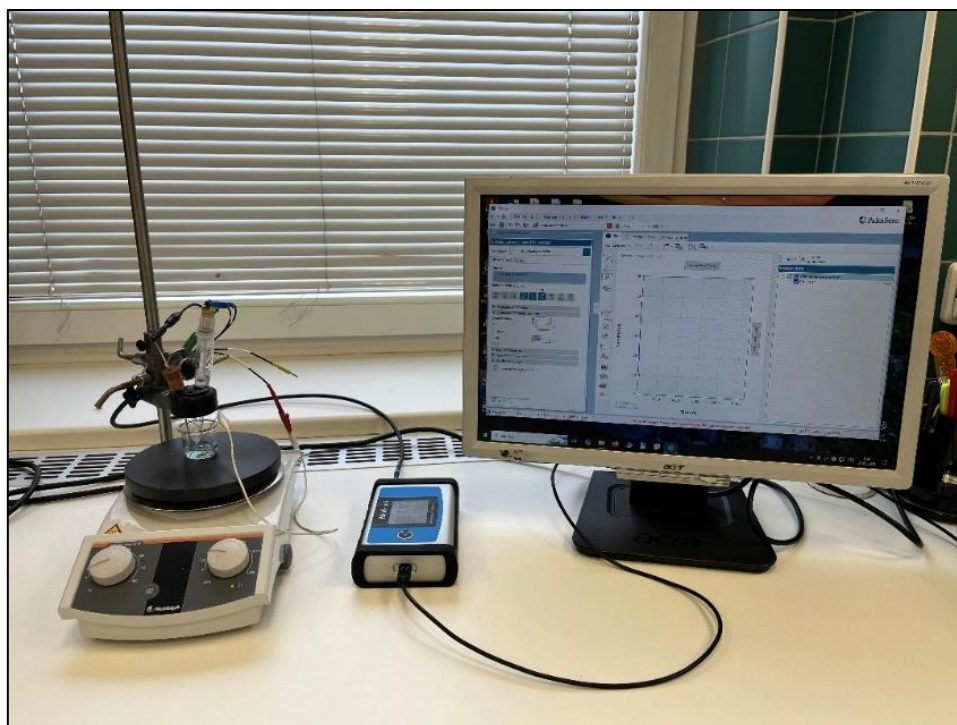


Figure 16 Apparatus for electrochemical analysis of MB [60]

The electrochemical cell was placed on a magnetic hotplate stirrer, which facilitated continuous mixing of the solution during the experiments. No gas was supplied during the experiments. The electrodes were connected to a PalmSens potentiostat via cable connectors with clips. The potentiostat was then linked to a computer for data acquisition and analysis. The complete apparatus is shown in Figure 17.



*Figure 17 Complete set-up for electrochemical analysis [60]*

### **3.5 Frequency optimization**

For analysing of the optimal frequency level, SWV was used. MB hydrate at a concentration of 5  $\mu\text{M}$  was adsorbed during one-minute at 250 RPM under open-circuit conditions (OCC) at a PGE used as the working electrode. The measurements were performed at room temperature, and the electrolyte consisted of NaCl with a pH of 10.22. The frequency was varied between 100 and 1500 Hz. No gas was supplied to the electrolyte during the measurements. The potential was scanned from -0.9 V to 1.3 V, with the oxidation process occurring in this potential range. The amplitude was set to 30 mV and the potential step was 5 mV.

### **3.6 Chronoamperometric measurement**

Chronoamperometric measurements were carried out to study the electrochemical degradation of MB solution. The experiment was performed at a constant potential of 1.3 V, with a time interval of 2 seconds and a total duration of 3 hours. The measurement was conducted under continuous stirring to ensure homogeneity of the solution. The initial concentration of MB solution was 2.5  $\mu\text{M}$  in a 4 mL volume of NaCl electrolyte. A PGE served as the working electrode, while an Ag|AgCl|3M KCl was used as the reference electrode. A platinum wire functioned as the auxiliary electrode. To assess the degradation process, the absorbance of the

MB solution was measured both before and after the chronoamperometric experiment by UV-VIS spectrophotometer. Chronoamperometry of MB was performed on both modified and unmodified electrodes.

### 3.7 Modification of the electrode surface

The modification of the PGE was performed using CV in 10 mM phosphoric acid ( $\text{H}_3\text{PO}_4$ ) solution. The process was carried out in 5 mL of  $\text{H}_3\text{PO}_4$ , with an applied potential range from -0.1 V to 2.1 V, a potential step of 5 mV, and a scan rate of 0.05 V/s. Only one scan was performed, with an equilibration time of 0 seconds before the scan. After the modification, the electrodes were briefly rinsed in triple-distilled water for a few seconds to remove excess acid. Thus, modified electrodes were prepared for electrochemical measurements.

The purpose of this modification was to enhance the electrochemical properties of graphite leads (used as working electrodes) by introducing oxygen-containing functional groups (-OH, -COOH, =O) onto the electrode surface to form graphite oxides (GrO). This improves charge transfer efficiency, surface hydrophilicity, and capacitive behaviour, making the electrode more suitable for some electrochemical analyses as well as for further modification [61].

After the modification of the electrode surface, it was characterized electrochemically using impedance spectroscopy by capacitance measurement of the electrode double layer,  $C$ , on  $E$  ( $C - E$  curves). The applied potential ranged from -0.8 V to 1.2 V with a step size of 0.01 V. The alternating current (ac) perturbation amplitude was set to 0.01 V, and the frequency used for measurements was 225.3 Hz. The minimum sampling time was 0.5 seconds, while the maximum equilibrium time was 0.01 seconds.

Figure 18 summarizes the characterization of unmodified and modified pencil PGE surface by scanning electron microscopy (SEM) (point A – D), X-ray photoelectron spectroscopy (XPS) (point E – F), Raman spectroscopy (point G – H) and by  $C - E$  curves (point I – J), reported in [61]. In the figure we can see that after modification, changes on the electrode surface occur, oxygen-containing groups are introduced (point E) and the capacity of the electrode increases (point I).

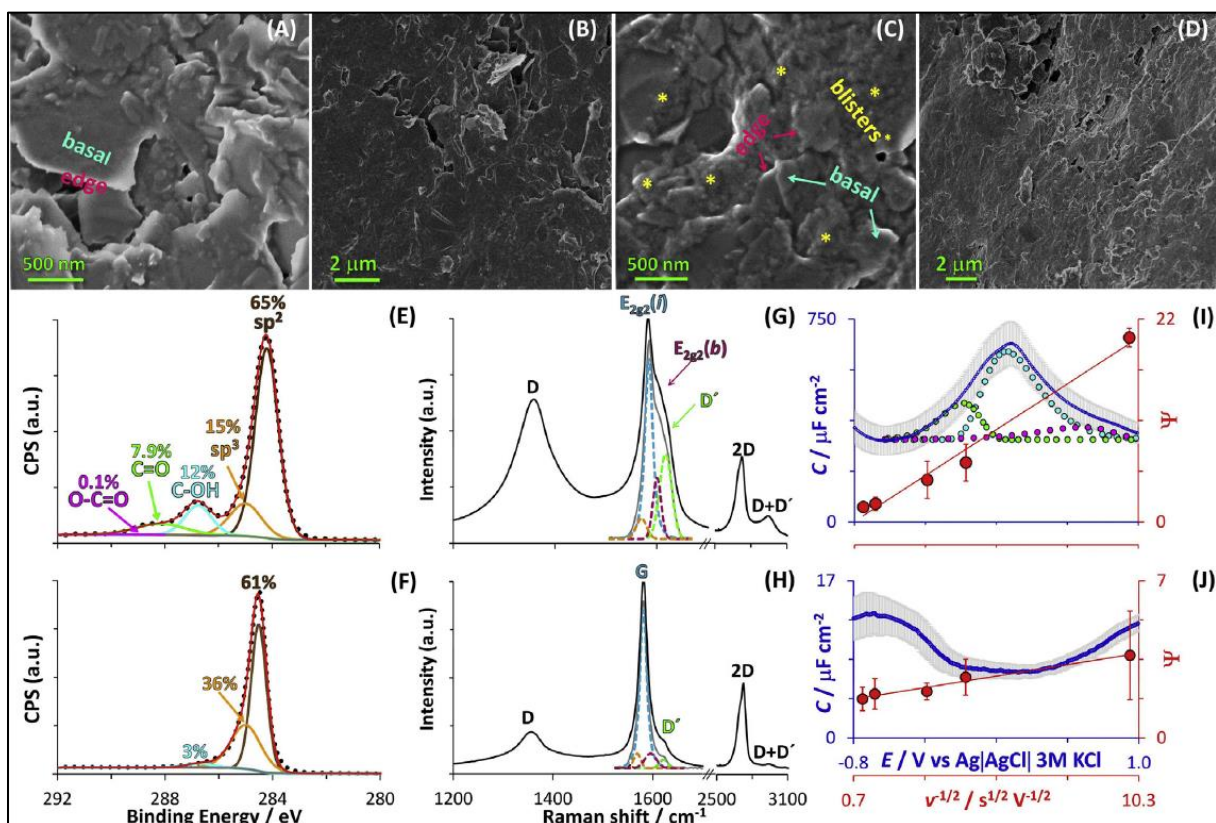


Figure 18 Characterization of unmodified and modified PGE [61]

### 3.8 Photocatalytic measurement

For photocatalytic measurement, 4 Eppendorf microtubes of 2 mL volume were used and 1.5 mL of a prepared 2.5  $\mu\text{M}$  MB solution in NaCl electrolyte. The microtubes were labelled and added as follows:

1. MB irradiated with 10  $\mu\text{L}$  of tri-distilled  $\text{H}_2\text{O}$
2. MB non-irradiated with 10  $\mu\text{L}$  of tri-distilled  $\text{H}_2\text{O}$
3. MB non-irradiated with 10  $\mu\text{L}$  of A-Na-TEG
4. MB irradiated with 10  $\mu\text{L}$  of A-Na-TEG.

Samples 1 - 3 served as reference samples for this experiment. In the beginning, the absorbance of solutions at the time zero was measured. The non-irradiated samples were placed in the dark at room temperature for 1 h. Irradiated samples were pipetted into quartz cuvettes with lids and placed for 1 h in a spectrofluorometer, where they were irradiated at 400 nm, which is the  $\lambda$  at which flavin A-Na-TEG absorbs EMR and produces ROS. During irradiation, the samples were often manually mixed due to non-use of the stirrer. After a period of 1 h, the absorbance of all samples was measured.

## 4. RESULTS AND DISCUSSION

The aim of this thesis was to develop a tandem method for wastewater treatment focused on the degradation of organic MPs. This approach combines two degradation processes - electrochemical oxidation and photocatalysis, using bio-photocatalysts capable of generating ROS, thereby enhancing the efficiency of pollutant breakdown.

MB was chosen as the model compound for degradation due to its electrochemical and spectrophotometric activity. The mechanism of MB degradation is partially described by Figure 14. A newly synthesized flavin, A-Na-TEG, was employed as the bio-photocatalyst in the photocatalytic process.

In order to develop this tandem method for micropollutant degradation, it was first necessary to test the two degradation mechanisms separately. The results of pilot experiments on these degradation processes are presented below.

### 4.1 Electrochemical degradation of MB

This section focuses on the first step of the tandem degradation of MB using electrochemical oxidation.

First, we focus on the electrochemical characterisation of MB. In Figure 19 we can observe the chemical structure of MB in its oxidized state (O) on the left side and reduced state (R) on the right side.

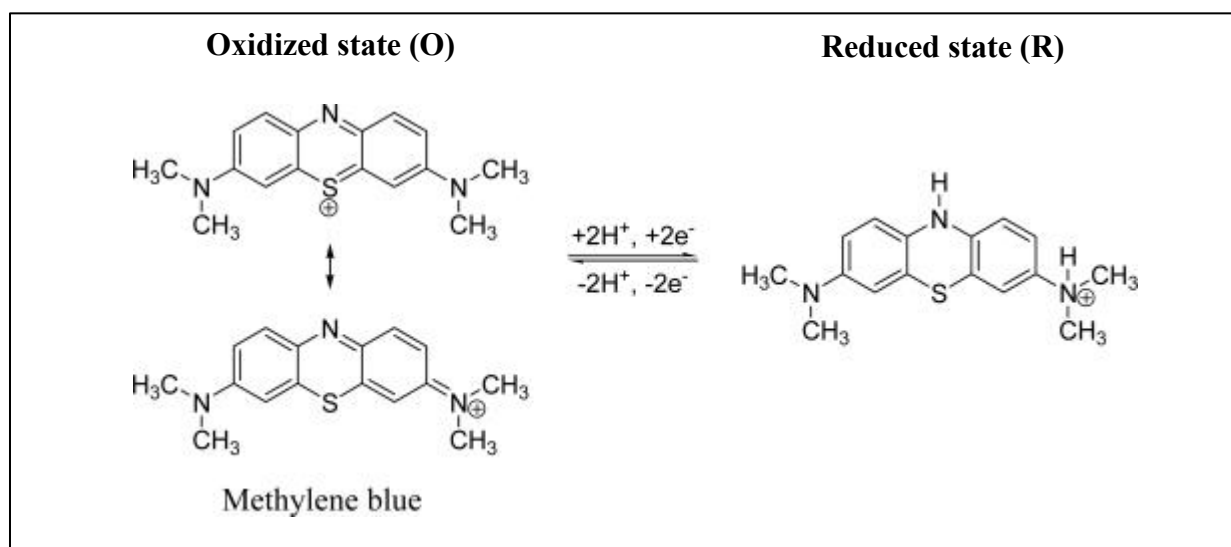
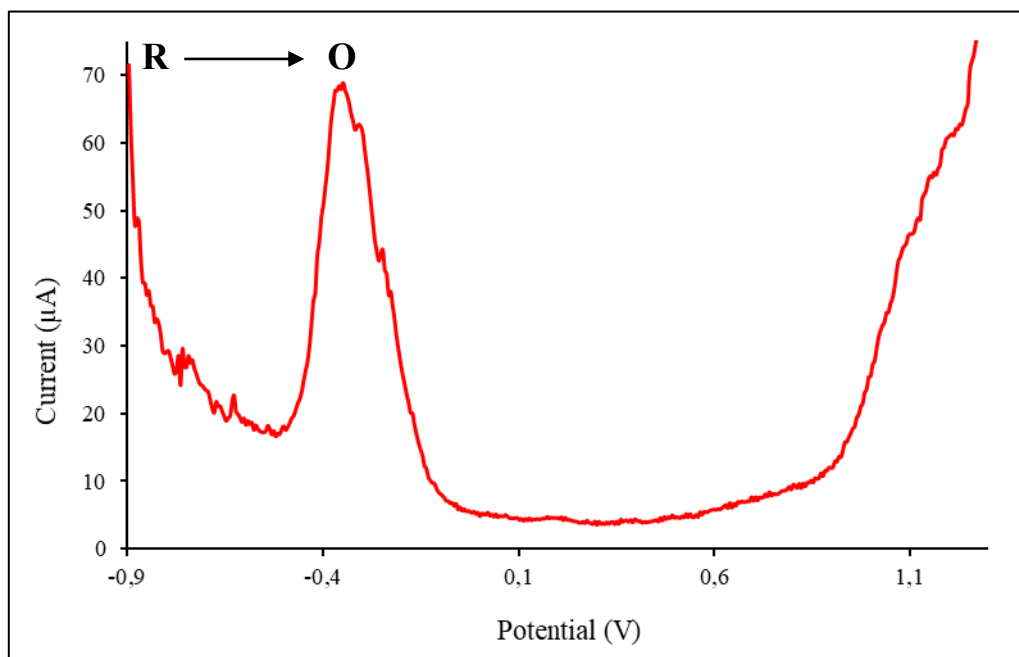


Figure 19 Oxidized and reduced state of MB, adapted from [62]

Figure 20 shows SW voltammogram of MB in the potential range from -0.9 to 1.3 V at a frequency of 100 Hz. MB was accumulated at a potential of -0.9 V, where it was present in reduced state (R). During the polarization, the potential value shifts to positive values, inducing MB oxidation (O). The oxidation is accompanied by well-developed voltametric peak with maximum at -0.3 V. Besides peak potential, oxidation process can be characterized by peak height and peak area. For the experiments a PGE was used as a working electrode for electron

transport between the MB and the surface of the electrode. We changed different parameters in SWV method to optimize conditions for subsequent experiments.



*Figure 20 SW voltammogram of MB*

#### **4.1.1 Frequency dependence**

Figure 21 shows the dependence of the oxidation peak area of MB on frequency. The peak area, measured as charge ( $\mu\text{C}$ ) passed across the interface, changes at different frequencies of the applied signal. As the frequency increases from 100 Hz, the peak area initially grows, which can be attributed to the increasing charge transfer, leading to better-developed signal. This growth is associated with faradaic processes, where efficient electron transfer dominates, allowing for optimal electrochemical detection. The peak area reaches its maximum at approximately 400 Hz ( $25 \mu\text{C}$ ), indicating the optimal balance between charge transfer kinetics and measurement conditions. However, at frequencies above 400 Hz, the peak area decreases because the charge transfer can no longer adequately follow the rapid potential changes, resulting in reduced measurement efficiency.

Although the maximum peak area occurs around 400 Hz, at 100 Hz the peak area remains sufficiently large, and this frequency offers several advantages. At low frequencies, such as 100 Hz, the signal is less affected by non-faradaic currents and noise, resulting in a cleaner and stable response. Additionally, the sensitivity at this frequency is still adequate, enabling reliable detection of the oxidation process. Higher frequencies, such as 500 Hz, may be more prone to errors caused by reaction kinetics or non-faradaic disturbances. At 100 Hz, the electrochemical system has enough time for the electrochemical reaction to proceed, which improves the stability and accuracy of quantitative analysis. For these reasons, 100 Hz was chosen as the optimal compromise between signal stability and sensitivity.

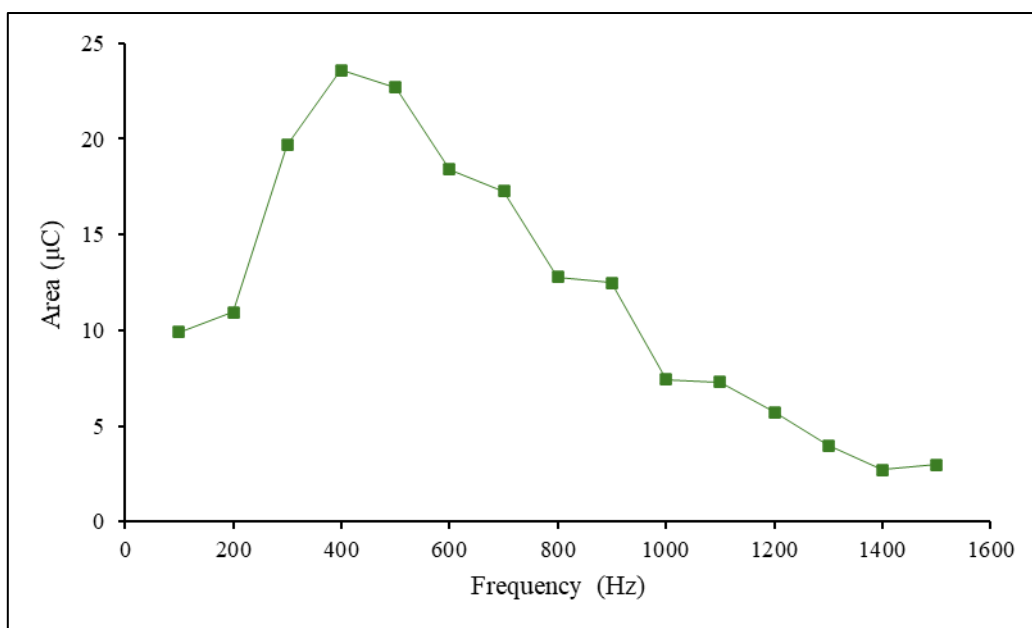


Figure 21 The dependence of peak area on frequency

#### 4.1.2 Concentration dependence

Figure 22 presents the dependence of peak height of MB on its concentration. The data points follow a trend where higher MB concentrations result in increased peak heights, indicating enhanced electrochemical activity and signal. This correlation suggests that the redox reaction of MB at the electrode surface is concentration-dependent, likely due to a greater number of electroactive molecules available for oxidation. This optimization was used to determine the concentration range at which further analysis will be performed.

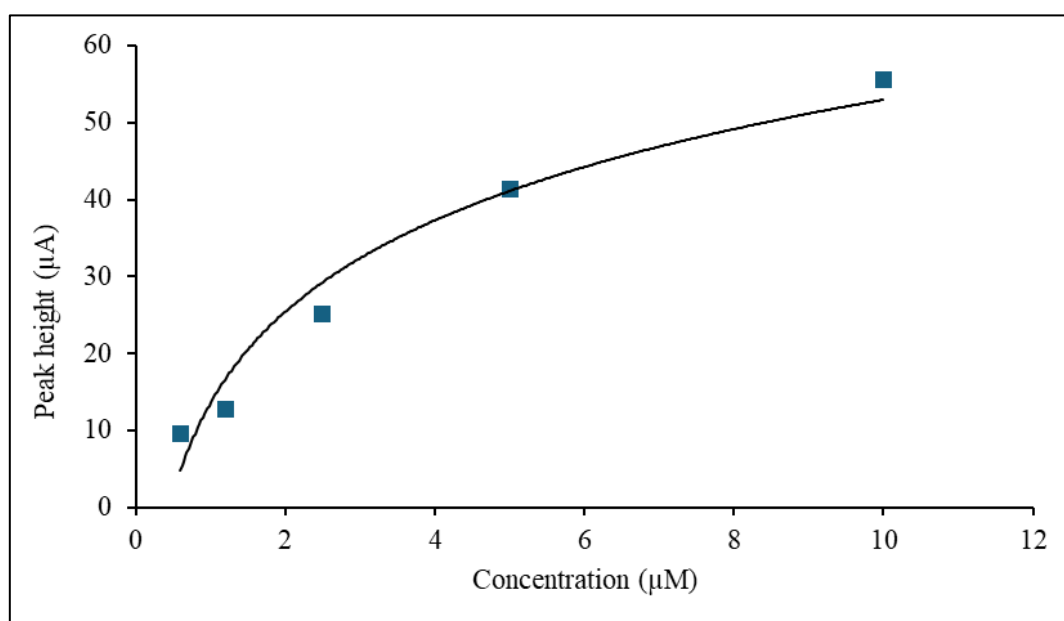


Figure 22 Peak height and MB concentration relation

### 4.1.3 Modification of the working electrode surface

In addition to the unmodified working electrode, an electrochemically modified version was prepared and characterized through capacitance measurements. The  $C-E$  curves illustrate the electrochemical capacitance of the electrode as a function of potential, see Figure 23. Comparing the two lines, the unmodified graphite electrode (red line) exhibits lower capacitance. In contrast, the modified electrode (blue line), treated with 0.1 M  $H_3PO_4$ , shows a significant increase in capacitance. The characterization of electrode surface after modification using  $C-E$  curves (reported in [61]) can be observed in Figure 18.

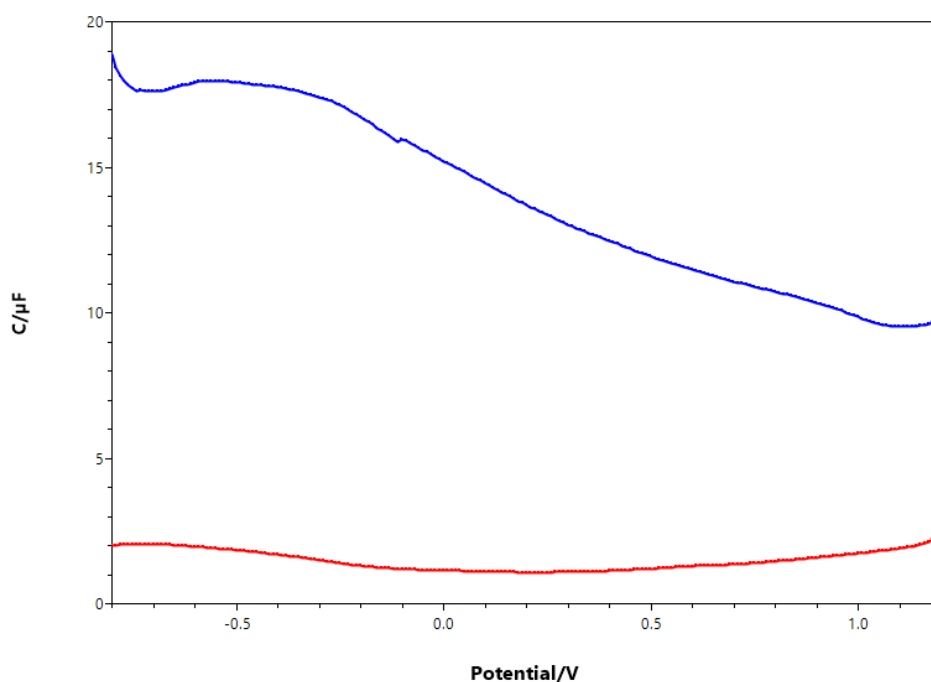


Figure 23  $C-E$  curves of unmodified (red line) and modified (blue line) PGE

The enhancement results from the formation of oxygen-containing functional groups on the electrode surface, which improve charge storage capability by providing more active sites for ion accumulation. The step increase in capacitance at positive potentials further confirms the improved electrochemical performance. The illustration of the GrO present on the electrode surface after modification can be seen in Figure 24.

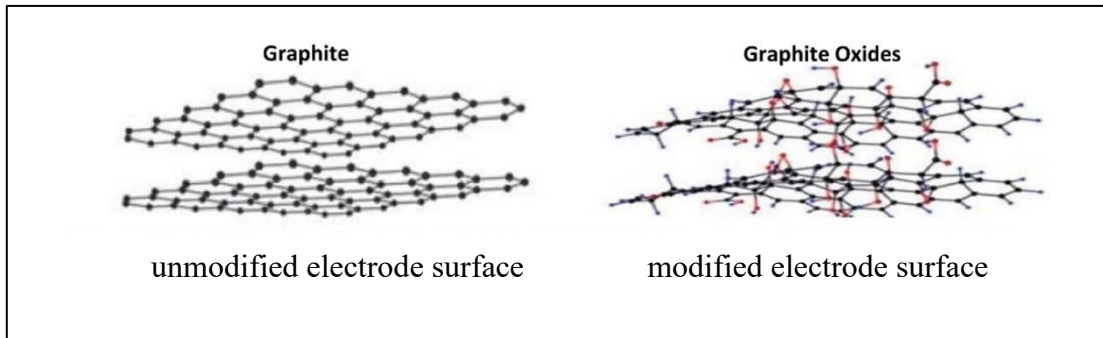


Figure 24 Formation of GrO on the electrode surface after its modification, adapted from [61]

Figure 25 shows the dependence of peak area ( $\mu\text{C}$ ) on analyte concentration ( $\mu\text{M}$ ) for both unmodified and modified electrode surfaces. It is evident that the modified electrode (orange points) exhibits significantly higher peak area values compared to the unmodified electrode (blue points) in whole range of concentrations. This trend indicates that the electrode surface modification led to a substantial increase in sensitivity and electrochemical response. The enhancement is due to an increase in the active surface area, improved analyte adsorption, or changes in surface properties, such as the introduction of oxygen-containing functional groups. As it is described in the literature [61], the modification of the electrode increases its active surface area due to the presence of low-molecular-weight (LMW) substances. LMW substances such as MB strongly adsorb at the electrode surface.

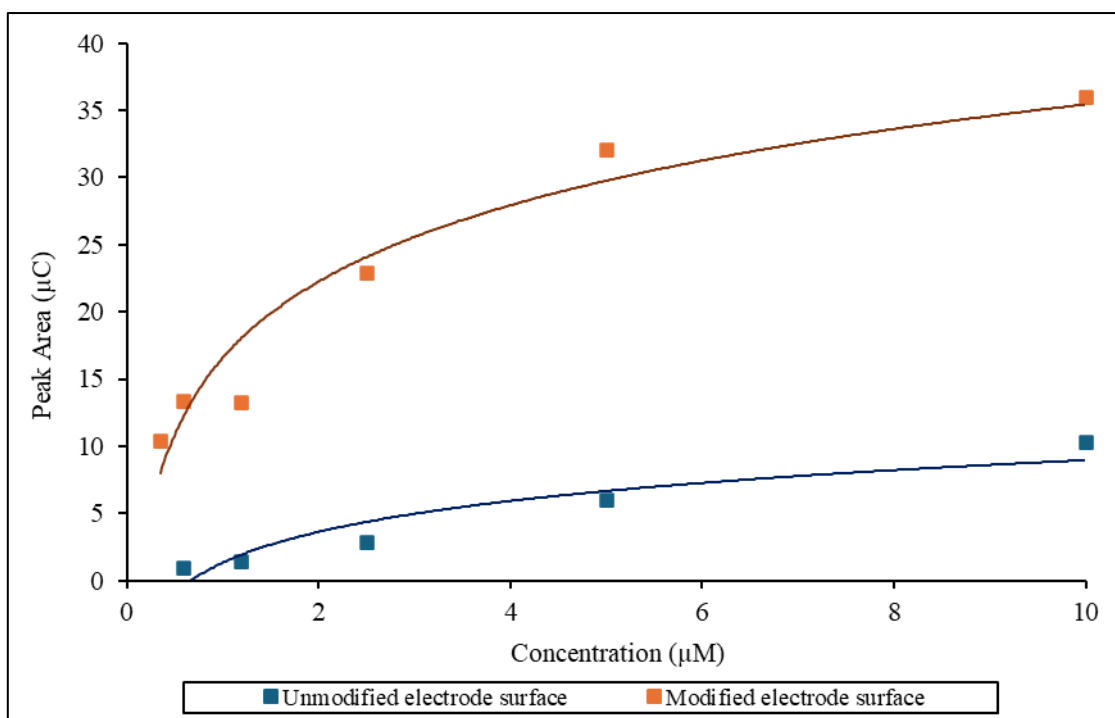


Figure 25 Comparison of transferred charge of MB at the modified and unmodified electrode surfaces

#### 4.1.4 Electrolysis of the MB solution using unmodified PGE

After MB characterization at unmodified and GrO-modified surfaces, experiments leading to the decomposition of MB using electrolysis were carried out. The electrolysis of MB involves its oxidation at the electrode surface at high positive potentials, leading to characteristic changes in current over time.

Figure 26 illustrates the chronoamperometric measurement of the electrolytic decomposition of MB solution at an applied potential of 1.3 V. The y-axis represents the current ( $\mu\text{A}$ ), while the x-axis shows the time (s). After an initial sharp decrease in current, a stabilization phase follows, likely due to the gradual depletion of the electroactive species near the electrode surface and the formation of a stable diffusion layer.

The experiment was conducted under stirring conditions, ensuring a homogeneous distribution of MB in the electrolyte. The shaded area under the current curve represents the total charge ( $Q$ ) transferred during the electrolysis. This charge can be calculated as the integral of the current over time and directly correlates with the amount of MB adsorbed onto the electrode surface.

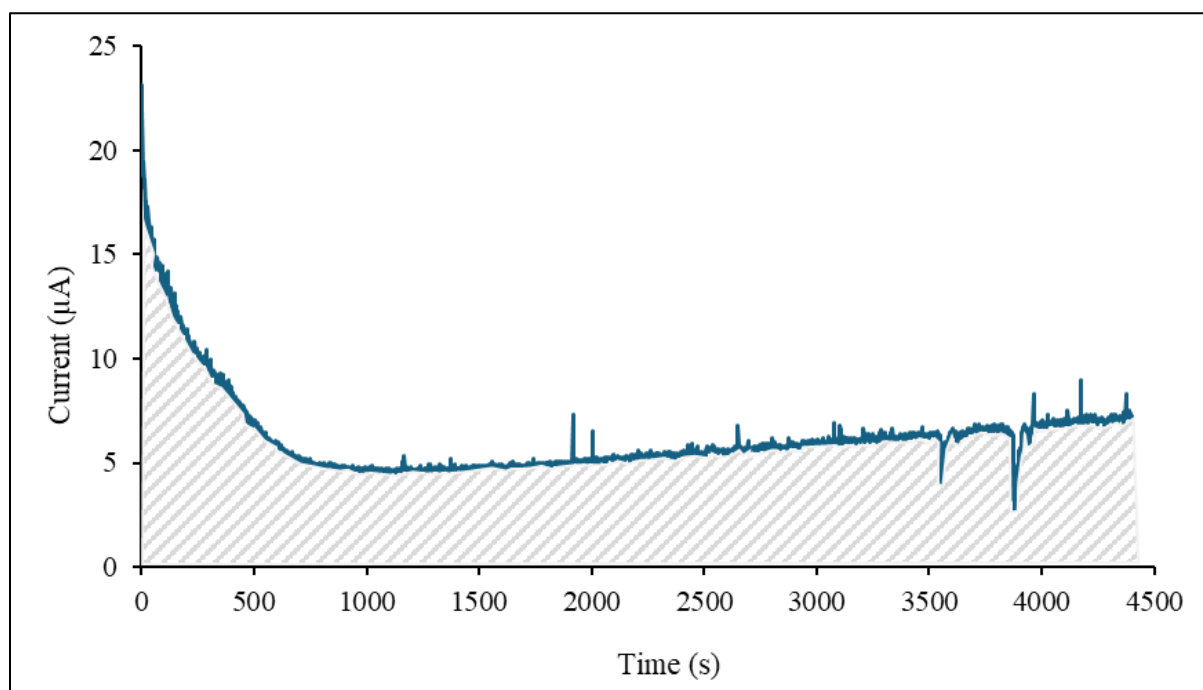


*Figure 26 Electrolysis of MB solution*

The effectiveness of electrolysis in degrading MB is demonstrated through changes in peak height and absorbance. Figure 27 illustrates the peak height ( $\mu\text{A}$ ) (on the left) and the absorbance (on the right) before and after electrolysis, showing a significant decrease after the process, which indicates the reduction of electroactive MB species.

Since both absorbance and peak height directly correlate with dye concentration, the results suggest successful electrochemical degradation of MB into simpler products with lower molar

mass. The resulting degradation products are not electrochemically active and do not provide spectrophotometric spectra. Possible degradation products of MB can be seen in Figure 14.

Future studies could employ Mass Spectrometry (MS) to identify the resulting degradation products. Investigating their toxicity would also be essential to validate the environmental safety of these methods, however it is not part of this master's thesis.

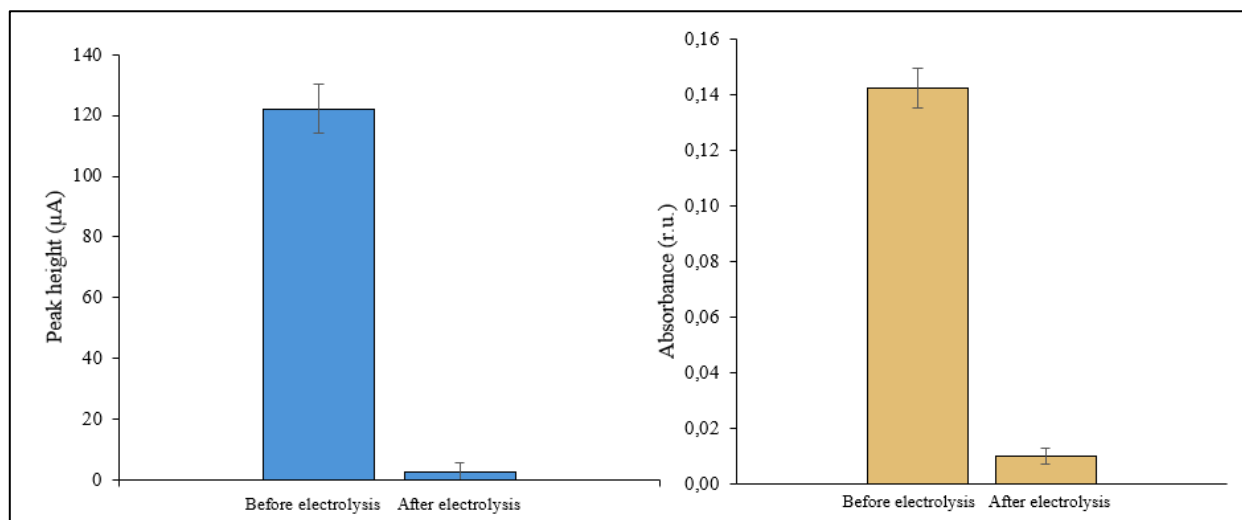


Figure 27 Reduction of peak height (left) and absorbance (right) after the electrolysis of MB

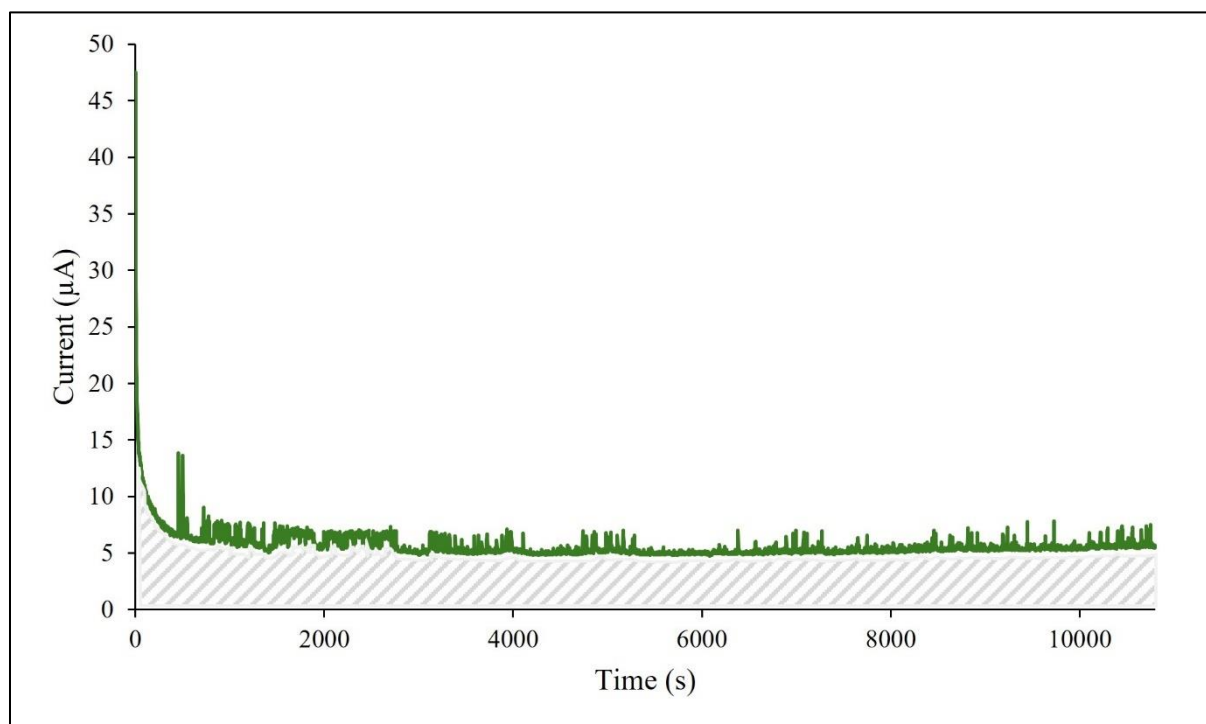
#### 4.1.5 Electrolysis of the MB solution using modified PGE

Figure 28 presents the chronoamperometric response of MB electrolysis using PGE modified by CV in 0.1 M phosphoric acid. The current response was recorded at a constant potential of 1.3 V over a total duration of 3 hours, with a sampling interval of 2 s under stirring conditions.

Initially, a high current was observed, peak height of approximately 45  $\mu\text{A}$ . Then rapidly decreased within the first few minutes. This initial sharp decline is likely due to the rapid depletion of electroactive MB molecules near the electrode surface as the redox reaction proceeds. As the experiment progresses, the current stabilizes at lower values around 5  $\mu\text{A}$ , indicating a steady-state conditions where the electrochemical reaction rate is limited by mass transport and diffusion of MB from the bulk solution.

The shaded area under the current curve represents the total charge transferred during the electrolysis. To assess the effectiveness of the electrode modification, the total transferred charge during electrolysis was calculated using Faraday's law. The results showed that 32 mC of charge was transferred when using the modified PGE, compared to 30 mC with the unmodified one. The difference is relatively small between MB degradation at both electrodes, which indicates that the modification of the PGE surface is effective for MB degradation. Compared to electrolysis using an unmodified PGE, the modified surface offers other advantages. It exhibits greater selectivity toward high molecular weight substances that do not adsorb onto the surface, thereby leaving active sites available for the adsorption and degradation of LMW compounds. Additionally, the functional groups introduced on the electrode surface

facilitate the incorporation of photocatalytic materials, potentially enhancing the overall efficiency of degradation processes in the tandem method.



*Figure 28 Electrolysis of MB solution using modified PGE*

Figure 29 illustrates the decrease in both absorbance and peak height of MB after electrolysis using a modified electrode. The absorbance of MB at 664 nm was initially 0.11 r.u. and dropped to 0.02 r.u. after electrolysis, indicating a significant reduction in MB concentration in solution. Similarly, the peak height in the electrochemical response decreased from 103  $\mu\text{A}$  to 34  $\mu\text{A}$ , reflecting a substantial decline in the amount of electroactive MB.

These results confirm the efficiency of the electrochemical process in degrading MB, as evidenced by both spectrophotometric and electrochemical measurements. The combined data suggest that the modified electrode facilitates MB oxidation, leading to its effective removal from the solution.

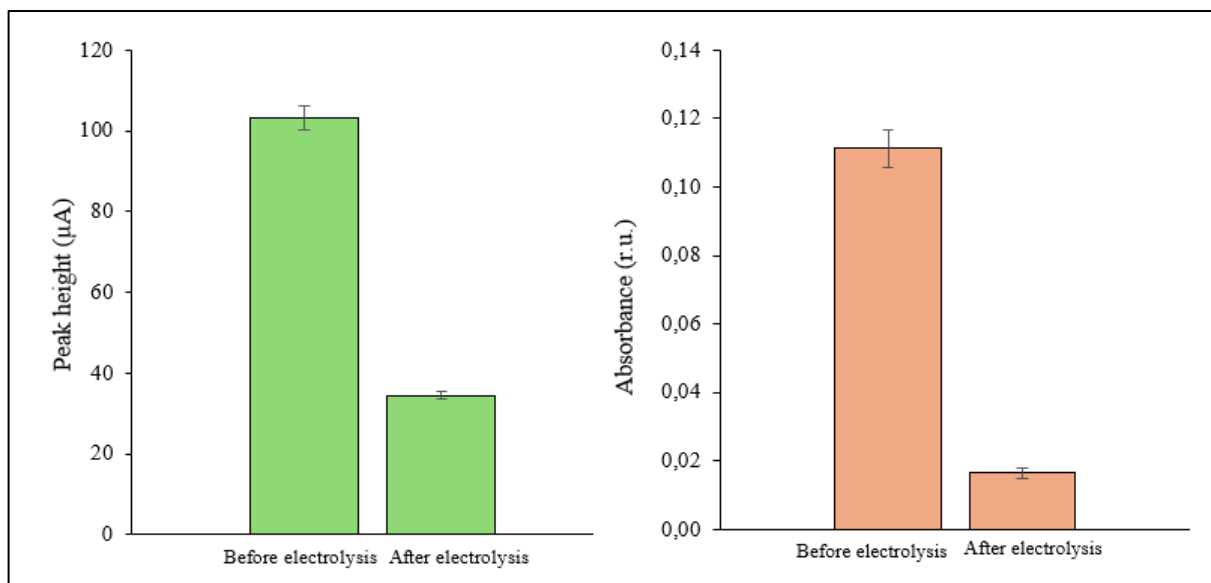


Figure 29 Reduction of peak height (left) and absorbance (right) after the electrolysis of MB on the modified electrode

## 4.2 Photocatalytic degradation of MB

This section focuses on the second part of the tandem degradation of MB using photocatalysis with flavin derivative A-Na-TEG.

The aim of this thesis is to design an approach based on the tandem removal of MPs by electrochemical oxidation and the degradation using ROS produced by an organic photocatalyst. Firstly, spectrophotometric characterization of newly synthesized flavin derivative A-Na-TEG and MB dye was carried out.

Flavin A-Na-TEG was synthesized by Ing. Lucia Ivanová Ph.D. from the Faculty of Chemistry, Brno University of Technology and was provided for the purpose of this master's thesis for tandem degradation of MB.

The basis for performing the spectrophotometric part of the experiment was the observation of the UV-VIS spectrum of the monitored substances in solution, namely the flavin derivative A-Na-TEG and MB. The joint spectrum is captured in Figure 30, the flavin is shown in orange and MB shown in blue. Flavin A-Na-TEG exhibits strong absorption in the UV to blue region of the spectrum, approximately from 200 to 420 nm, while MB absorbs in the VIS region from 550 to 700 nm. The x-axis represents the  $\lambda$  (nm), while the y-axis shows the absorbance (r.u.).

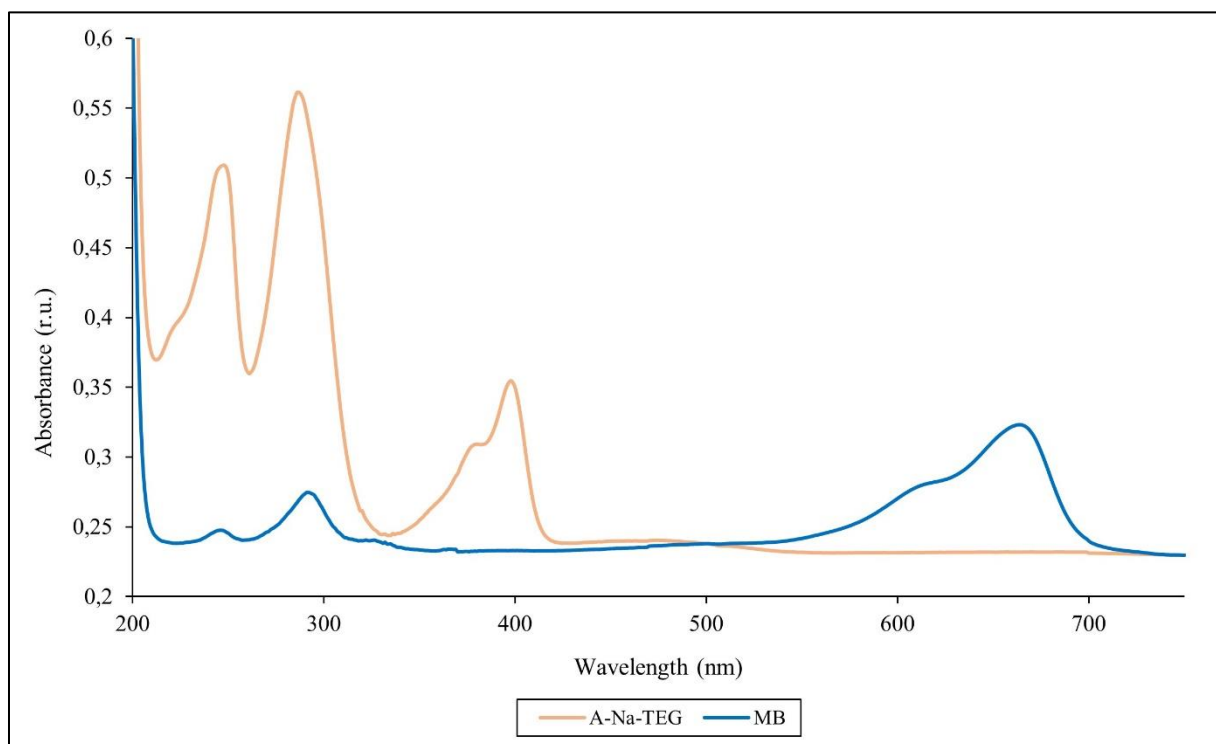


Figure 30 Spectrum of the A-Na-TEG (orange) and MB (blue)

A-Na-TEG exhibits a maximum absorption peak at 398 nm, while MB shows its peak at 664 nm. For ROS production, samples were irradiated at 400 nm, and the results were assessed at 664 nm.

The results of photocatalytic measurements of the samples can be seen in Figure 31. It can be noticed that for samples containing MB only, whether irradiated or not, there was no decrease in the absorbance of the sample and therefore no decrease in its concentration.

On the other hand, the samples containing both MB and A-Na-TEG exhibited a slight but noticeable decrease in absorbance under irradiation. This decrease is directly proportional to the decrease of the MB concentration, indicating that the photocatalytic process was occurring. During irradiation, light-driven ROS production by the A-Na-TEG molecules arises, which partially degrades the MB molecules.

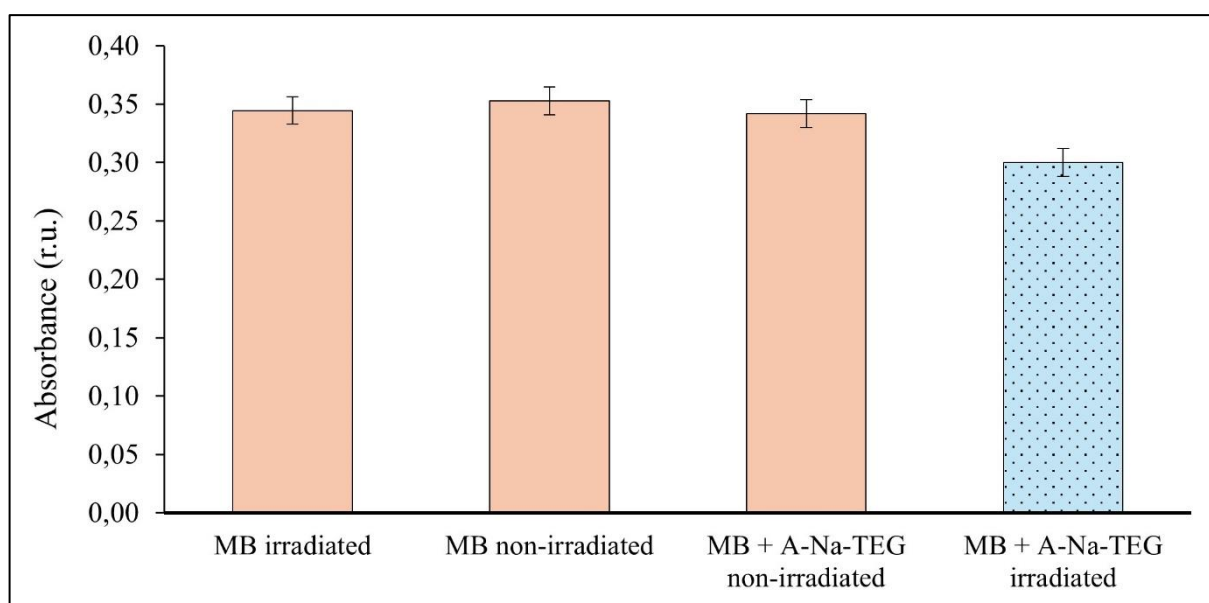


Figure 31 Irradiated and non-irradiated MB and A-Na-TEG samples at 400 nm

A-Na-TEG was expected to photocatalytically degrade MB into simpler, non-toxic byproducts such as CO<sub>2</sub> and water. However, the observed reduction in MB concentration was lower than anticipated.

To conclude this section, while a decrease in absorbance was observed in the presence of A-Na-TEG, its resulting extent cannot be considered as sufficient. This suggests that further enhancement of the experimental conditions is necessary to achieve higher degradation efficiency. Additionally, optimization of current flavin molecule or exploring alternative flavin derivatives, could lead to better photocatalytic activity and further improvement of the efficiency of the process. Also, the efficiency of this process could be further improved by directly binding the flavin derivative to the electrode surface.

## 5. CONCLUSION

This master's thesis focuses on the design and development of a tandem method of wastewater treatment using electrochemical oxidation and photocatalysis for the degradation of MPs, representing a potential quaternary stage of wastewater treatment. This thesis deals with pilot tests of these two separate processes that could subsequently be tandemly coupled in such a manner.

The experimental part of this thesis focused on two key degradation mechanisms: electrochemical oxidation driven by applied voltage/current and photocatalytic generation of ROS using organic photocatalysts. A significant advantage of this method lies in its use of cost-effective and widely available materials, such as PG as the working electrode and organic nature-inspired photocatalysts. This synergy not only improves pollutant degradation but also minimizes overall energy consumption, making the approach both economically and environmentally sustainable.

During the study, MB was used as a model compound, enabling both electrochemical and spectrophotometric monitoring of its degradation. The AO of MB was carried out in two ways, using unmodified and oxygen-containing functional groups-modified PGE to improve its electrochemical properties. The effectiveness of the MB electrolysis was validated by measuring the peak height and absorbance before and after AO treatment. In the sample after electrolysis, there was a significant decrease in both measured parameters, corresponding to an overall decrease in the concentration of MB in solution. We expect that MB has been degraded by electrolysis to simpler products. However, the identification of degradation products will be determined by MS in the next step.

Additionally, the ability of a newly synthesized flavin derivative, A-Na-TEG, to generate ROS and facilitate MB degradation was tested. The samples exhibited only a slight decrease in absorbance under irradiation. This decrease is directly proportional to the reduction in the concentration of MB, indicating that the photocatalytic process was occurring, but must be further optimized.

The obtained data demonstrate that both AO and ROS production by flavin derivative A-Na-TEG are functional, supporting the feasibility of the proposed innovative wastewater treatment strategy. These findings suggest that this method could have strong potential for further development as an effective and energy-efficient wastewater purification strategy. However, future research should focus on optimizing A-Na-TEG molecule or another flavin derivative modifications to achieve higher ROS yields and improve their stability, as well as exploring effective methods for immobilizing flavins onto the PGE surface.

## 6. REFERENCES

- [1] ALMAZROUEI, Balqees; ISLAYEM, Deema; ALSKAFI, Feryal; CATA CUTAN, Mary Krystelle; AMNA, Riffat et al. Steroid hormones in wastewater: Sources, treatments, environmental risks, and regulations. Online. *Emerging Contaminants*. 2023, roč. 9, č. 2. ISSN 24056650. Dostupné z: <https://doi.org/10.1016/j.emcon.2023.100210>. [cit. 2023-12-13].
- [2] LI, Hongxiang; ZHAO, Kun; ZHANG, Xiaoxia; YU, Hongtao; WANG, Jianbing et al. Electrochemical Anodic Oxidation-Based Membrane System for Micropollutant Removal. Online. *ACS Publications*. 2023, roč. 4, č. 2. Dostupné z: <https://doi.org/https://doi.org/10.1021/acsestengg.3c00380>. [cit. 2024-08-21].
- [3] EUROPEAN PARLIAMENT, COUNCIL OF THE EUROPEAN UNION. *Directive (EU) 2024/3019 of the European Parliament and of the Council of 27 November 2024 concerning urban wastewater treatment*. Online. In: EUROPEAN UNION. EUR-Lex. 2024. Dostupné z: <https://eur-lex.europa.eu/legal-content/EN/TXT/?uri=CELEX:32024L3019>. [cit. 2025-01-28].
- [4] PAVANELLO, Alice; FABBRI, Debora; CALZA, Paola; BATTISTON, Debora; MIRANDA, Miguel A. et al. Photocatalytic degradation of drugs in water mediated by acetylated riboflavin and visible light: A mechanistic study. Online. *Journal of Photochemistry and Photobiology B: Biology*. 2021, roč. 221. ISSN 10111344. Dostupné z: <https://doi.org/10.1016/j.jphotobiol.2021.112250>. [cit. 2025-03-15].
- [5] OTURAN, Mehmet A. a AARON, Jean-Jacques. Advanced Oxidation Processes in Water/Wastewater Treatment: Principles and Applications. A Review. Online. *Critical Reviews in Environmental Science and Technology*. 2014, roč. 44, č. 23, s. 2577-2641. ISSN 1064-3389. Dostupné z: <https://doi.org/10.1080/10643389.2013.829765>. [cit. 2025-03-16].
- [6] ZAVISKA, François; DROGUI, Patrick; BLAIS, Jean-François a MERCIER, Guy. In situ active chlorine generation for the treatment of dye-containing effluents. Online. *Journal of Applied Electrochemistry*. 2009, roč. 39, č. 12, s. 2397-2408. ISSN 0021-891X. Dostupné z: <https://doi.org/10.1007/s10800-009-9927-x>. [cit. 2025-03-18].
- [7] RIFFAT, Rumana a HUSNAIN, Taqsim. *Fundamentals of Wastewater Treatment and Engineering*. Online. 2nd ed. United Kingdom: CRC Press, 2022. ISBN 978-1-003-13437-4. Dostupné z: <https://doi.org/10.1201/9781003134374>. [cit. 2025-03-11].
- [8] ČESKÁ REPUBLIKA. *Zákon č. 254/2001 Sb.: Zákon o vodách a o změně některých zákonů (vodní zákon)*. Online. In: AION CS, S.R.O. *Zákony pro lidi*. 2024. Dostupné z: <https://www.zakonyprolidi.cz/cs/2001-254/zneni-20240801>. [cit. 2025-03-11].

- [9] DAS, Sreejon; MITRA RAY, Nillohit; WAN, Jing; KHAN, Adnan; CHAKRABORTY, Tulip et al. Micropollutants in Wastewater: Fate and Removal Processes. In: FAROOQ, Robina a AHMAD, Zaki. *Physico-Chemical Wastewater Treatment and Resource Recovery*. Pakistan: BoD – Books on Demand, 2017, s. 75-108. ISBN 978-953-51-3130-4.
- [10] OPEN LEARN. *Flow diagram of the stages of treatment in a sewage treatment plant*. Online. In: The Open University. Dostupné z: <https://www.open.edu/openlearn/nature-environment/environmental-studies/understanding-water-quality/content-section-5.1>. [cit. 2025-04-11].
- [11] PISTOCCHI, A.; ANDERSEN, H.R.; BERTANZA, G.; BRANDER, A.; CHOUBERT, J.M. et al. Treatment of micropollutants in wastewater: Balancing effectiveness, costs and implications. Online. *Science of The Total Environment*. 2022, roč. 850. ISSN 00489697. Dostupné z: <https://doi.org/10.1016/j.scitotenv.2022.157593>. [cit. 2025-03-11].
- [12] EGGEN, Rik I. L.; HOLLENDER, Juliane; JOSS, Adriano; SCHÄRER, Michael a STAMM, Christian. Reducing the Discharge of Micropollutants in the Aquatic Environment: The Benefits of Upgrading Wastewater Treatment Plants. Online. 2014, roč. 48, č. 14, s. 7683-7689. ISSN 0013-936X. Dostupné z: <https://doi.org/10.1021/es500907n>. [cit. 2025-03-13].
- [13] NAWAZ, Tabish; SENGUPTA, Sukalyan a AHUJA, Satinder. Contaminants of Emerging Concern: Occurrence, Fate, and Remediation. Online. In: *Advances in Water Purification Techniques*. Elsevier, 2019, s. 67-114. ISBN 978-0-12-814790-0. Dostupné z: [https://www.researchgate.net/publication/330339028\\_Contaminants\\_of\\_Emerging\\_Concern\\_Occurrence\\_Fate\\_and\\_Remediation](https://www.researchgate.net/publication/330339028_Contaminants_of_Emerging_Concern_Occurrence_Fate_and_Remediation). [cit. 2025-03-13].
- [14] KUMAR GAUTAM, Ravindra a CHANDRA CHATTOPADHYAYA, Mahesh. *Nanomaterials for Wastewater Remediation*. Online. Elsevier, 2016. ISBN 9780128047415. Dostupné z: <https://doi.org/10.1016/B978-0-12-804609-8.00002-9>. [cit. 2025-03-13].
- [15] MUNTER, R. ADVANCED OXIDATION PROCESSES – CURRENT STATUS AND PROSPECTS. Online. *Proceedings of the Estonian Academy of Sciences. Chemistry*. 2001, roč. 50, č. 2. ISSN 1406-0124. Dostupné z: <https://doi.org/10.3176/chem.2001.2.01>. [cit. 2025-03-15].
- [16] BIBI, Amina; BIBI, Shazia; ABU-DIEYEH, Mohammed a AL-GHOUTI, Mohammad A. Towards sustainable physiochemical and biological techniques for the remediation of phenol from wastewater: A review on current applications and removal mechanisms. Online. *Journal of Cleaner Production*. 2023, roč. 417. ISSN 09596526. Dostupné z: <https://doi.org/10.1016/j.jclepro.2023.137810>. [cit. 2025-03-15].

- [17] IHSAN, Awais Ullah; KHAN, Farhan Ullah; KHONGORZUL, Puregmaa; AHMAD, Khalil Ali; NAVEED, Muhammad et al. Role of oxidative stress in pathology of chronic prostatitis/chronic pelvic pain syndrome and male infertility and antioxidants function in ameliorating oxidative stress. Online. 2018, roč. 106, s. 714-723. ISSN 07533322. Dostupné z: <https://doi.org/10.1016/j.biopha.2018.06.139>. [cit. 2025-03-16].
- [18] AAT BIOQUEST, INC. *Reactive Oxygen Species (ROS)*. Online. In: AAT BIOQUEST. Dostupné z: <https://www.aatbio.com/catalog/reactive-oxygen-species-ros-indicators-probes-quantification-kits>. [cit. 2025-04-24].
- [19] SOLARCHEM ENVIRONMENTAL SYSTEMS. *The UV/Oxidation Handbook*. Online. Canada, 1994. Dostupné z: <https://p2infohouse.org/ref/27/26568.pdf>. [cit. 2025-03-18].
- [20] MAZILLE, Félicien. *Main steps involved in an AOPs treatment of wastewater containing toxic organic compounds*. Online. In: Sustainable Sanitation and Water Management Toolbox. 2011. Dostupné z: <https://sswm.info/sswm-university-course/module-6-disaster-situations-planning-and-preparedness/further-resources-0/advanced-oxidation-processes>. [cit. 2025-03-18].
- [21] DA POZZO, Anna; MERLI, Carlo; SIRÉS, Ignasi; GARRIDO, José Antonio; RODRÍGUEZ, Rosa María et al. Removal of the herbicide amitrole from water by anodic oxidation and electro-Fenton. Online. *Environmental Chemistry Letters*. 2005, roč. 3, č. 1, s. 7-11. ISSN 1610-3653. Dostupné z: <https://doi.org/10.1007/s10311-005-0104-0>. [cit. 2025-04-06].
- [22] NEYENS, E. a BAEYENS, J. A review of classic Fenton's peroxidation as an advanced oxidation technique. Online. *Journal of Hazardous Materials*. 2003, roč. 98, č. 1-3, s. 33-50. ISSN 03043894. Dostupné z: [https://doi.org/10.1016/S0304-3894\(02\)00282-0](https://doi.org/10.1016/S0304-3894(02)00282-0). [cit. 2025-04-06].
- [23] BARD, Allen J. a FAULKNER, Larry R. *Electrochemical methods: fundamentals and applications*. Online. 2nd ed. New York: Wiley, 2001. ISBN 04-710-4372-9.
- [24] VACEK, Jan a OSTATNÁ, Veronika. *Bioelektrochemie*. Olomouc: Univerzita Palackého v Olomouci, 2020. ISBN 978-802-4457-642.
- [25] WANG, Joseph. *Analytical electrochemistry*. Third edition. Hoboken: Wiley-VCH, [2006]. ISBN 04-716-7879-1.
- [26] HARVEY, David. *Electrochemical Cell for Voltammetry*. Online. In: . 2013. Dostupné z: <https://asplib.org/imageandvideoexchange/forum/electrochemical-cell-for-voltammetry/>. [cit. 2024-08-29].

- [27] MARUCCIO, Giuseppe a NARANG, Jagriti (ed.). *Electrochemical Sensors*. United Kingdom: Woodhead Publishing, 2022. ISBN 978-0-12-823148-7.
- [28] GRYGAR, Tomáš; MARKEN, Frank; SCHRÖDER, Uwe a SCHOLZ, Fritz. Electrochemical Analysis of Solids. A Review. Online. *Collection of Czechoslovak Chemical Communications*. 2002, roč. 67, č. 2, s. 163-208. ISSN 0010-0765. Dostupné z: <https://doi.org/10.1135/cccc20020163>. [cit. 2024-09-07].
- [29] NAVRATIL, Rudolf; KOTZIANOVA, Adela; HALOUZKA, Vladimir; OPLETAL, Tomas; TRISKOVA, Iveta et al. Polymer lead pencil graphite as electrode material: Voltammetric, XPS and Raman study. Online. *Journal of Electroanalytical Chemistry*. 2016, roč. 783, s. 152-160. ISSN 15726657. Dostupné z: <https://doi.org/10.1016/j.jelechem.2016.11.030>. [cit. 2024-09-07].
- [30] ANNU; SHARMA, Swati; JAIN, Rajeev a RAJA, Antony Nitin. Review—Pencil Graphite Electrode: An Emerging Sensing Material. Online. *Journal of The Electrochemical Society*. 2019, roč. 167, č. 3. ISSN 0013-4651. Dostupné z: <https://doi.org/10.1149/2.0012003JES>. [cit. 2025-03-20].
- [31] EINAGA, Yasuaki. Boron-Doped Diamond Electrodes: Fundamentals for Electrochemical Applications. Online. *Accounts of Chemical Research*. 2022, roč. 55, č. 24, s. 3605-3615. ISSN 0001-4842. Dostupné z: <https://doi.org/10.1021/acs.accounts.2c00597>. [cit. 2024-09-24].
- [32] HRDLÍČKA, Vojtěch; MATVIEIEV, Oleksandr; NAVRÁTIL, Tomáš a ŠELEŠOVSKÁ, Renáta. Recent advances in modified boron-doped diamond electrodes: A review. Online. *Electrochimica Acta*. 2023, roč. 456. ISSN 00134686. Dostupné z: <https://doi.org/10.1016/j.electacta.2023.142435>. [cit. 2024-09-24].
- [33] METROHM. *Copper working electrode 5 mm*. Online. In: Metrohm. Dostupné z: [https://www.metrohm.com/cs\\_cz/products/r/de\\_c/rde\\_cu50\\_s.html](https://www.metrohm.com/cs_cz/products/r/de_c/rde_cu50_s.html). [cit. 2025-04-11].
- [34] BRETT, Christopher a BRETT, Ana Maria Oliveira. *Electrochemistry: Principles, Methods, and Applications*. United States: Oxford University Press, 1993. ISBN 0198553889.
- [35] HONEYCHURCH, K.C. Printed thick-film biosensors. Online. *Printed Films*. 2012, s. 366-409. ISBN 9781845699888. Dostupné z: <https://doi.org/10.1533/9780857096210.2.366>. [cit. 2024-10-15].
- [36] ISLAM, Md. Nazmul a CHANNON, Robert B. Electrochemical sensors. Online. *Bioengineering Innovative Solutions for Cancer*. 2020, s. 47-71. ISBN 9780128138861. Dostupné z: <https://doi.org/10.1016/B978-0-12-813886-1.00004-8>. [cit. 2025-01-16].

- [37] WANG, JIAN LONG a XU, LE JIN. Advanced Oxidation Processes for Wastewater Treatment: Formation of Hydroxyl Radical and Application. Online. *Critical Reviews in Environmental Science and Technology*. 2012, roč. 42, č. 3, s. 251-325. ISSN 1064-3389. Dostupné z: <https://doi.org/10.1080/10643389.2010.507698>. [cit. 2025-03-20].
- [38] KOUNAVES, Samuel P. a SETTLE, Frank A. Voltammetric Techniques. Online. In: *Handbook of Instrumental Techniques for Analytical Chemistry*. Prentice Hall PTR, 1997, s. 709-725. ISBN 0131773380. Dostupné z: [https://diverdi.colostate.edu/all\\_courses/handbook%20of%20instrumental%20techniques%20for%20analysis/ch37.pdf](https://diverdi.colostate.edu/all_courses/handbook%20of%20instrumental%20techniques%20for%20analysis/ch37.pdf). [cit. 2024-10-28].
- [39] ELGRISHI, Noémie; ROUNTREE, Kelley J.; MCCARTHY, Brian D.; ROUNTREE, Eric S.; EISENHART, Thomas T. et al. A Practical Beginner's Guide to Cyclic Voltammetry. Online. *Journal of Chemical Education*. 2018, roč. 95, č. 2, s. 197-206. ISSN 0021-9584. Dostupné z: <https://doi.org/10.1021/acs.jchemed.7b00361>. [cit. 2024-10-30].
- [40] MIRCESKI, Valentin a GULABOSKI, Rubin. *Recent Achievements In Square-Wave Voltammetry (a review)*. Online. [Skopje]: Society of Chemists and Technologists of Macedonia, 2014. ISBN 1857-5625. Dostupné z: <http://eprints.ugd.edu.mk/9978/1/Square-wave%20voltammetry-Review%20in%20MJCCE%202014.pdf>. [cit. 2024-11-17].
- [41] KATIPAMULA, Sriram; WHITE, Navar M. a WALDIE, Kate M. Controlled-potential electrolysis for evaluating molecular electrocatalysts. Online. *Chem Catalysis*. 2023, roč. 3, č. 3. ISSN 26671093. Dostupné z: <https://doi.org/10.1016/j.cheecat.2023.100561>. [cit. 2025-01-19].
- [42] AHTASHAM IQBAL, Muhammad; AKRAM, Sumia; KHALID, Shahreen; LAL, Basant; HASSAN, Sohaib UI et al. Advanced photocatalysis as a viable and sustainable wastewater treatment process: A comprehensive review. Online. *Environmental Research*. 2024, roč. 253. ISSN 00139351. Dostupné z: <https://doi.org/10.1016/j.envres.2024.118947>. [cit. 2025-03-24].
- [43] AMETA, Rakshit; SOLANKI, Meenakshi S.; BENJAMIN, Surbhi a AMETA, Suresh C. Photocatalysis. Online. *Advanced Oxidation Processes for Waste Water Treatment*. 2018, s. 135-175. ISBN 9780128104996. Dostupné z: <https://doi.org/10.1016/B978-0-12-810499-6.00006-1>. [cit. 2025-03-24].
- [44] KOIPPULLY MANIKANDAN, Soumya; SHILLI, Anuradha; NORONHA, Florence Ruth a NAIR, Vaishakh. *Schematic illustration on decomposition of pesticide by TiO2 photocatalysis*. Online. In: Science Direct. 2022. Dostupné z: <https://www.sciencedirect.com/topics/earth-and-planetary-sciences/photocatalysis>. [cit. 2025-03-27].

- [45] LI, Chunmei; XU, You; TU, Wenguang; CHEN, Gang a XU, Rong. Metal-free photocatalysts for various applications in energy conversion and environmental purification. Online. *Green Chemistry*. 2017, roč. 19, č. 4, s. 882-899. ISSN 1463-9262. Dostupné z: <https://doi.org/10.1039/C6GC02856J>. [cit. 2025-03-27].
- [46] MARTINEZ-HAYA, Rebeca; MIRANDA, Miguel A. a MARIN, M. Luisa. Metal-Free Photocatalytic Reductive Dehalogenation Using Visible-Light: A Time-Resolved Mechanistic Study. Online. *European Journal of Organic Chemistry*. 2017, roč. 2017, č. 15, s. 2164-2169. ISSN 1434-193X. Dostupné z: <https://doi.org/10.1002/ejoc.201601494>. [cit. 2025-03-27].
- [47] BURGESS, C. Chapter 1 The basics of spectrophotometric measurement. Online. In: *UV-Visible Spectrophotometry of Water and Wastewater. Techniques and Instrumentation in Analytical Chemistry*. Elsevier, 2007, s. 1-19. ISBN 9780444530929. Dostupné z: [https://doi.org/10.1016/S0167-9244\(07\)80003-5](https://doi.org/10.1016/S0167-9244(07)80003-5). [cit. 2025-02-18].
- [48] SAJID HAMID AKASH, Muhammad a REHMAN, Kanwal. *Essentials of Pharmaceutical Analysis*. Online. Springer Nature Singapore Pte, 2019. ISBN 9789811515460. Dostupné z: <https://doi.org/https://doi.org/10.1007/978-981-15-1547-7>. [cit. 2025-02-20].
- [49] VALEUR, Bernard a BROCHON, Jean-Claude. *New Trends in Fluorescence Spectroscopy: Applications to Chemical and Life Sciences*. Online. Springer Science & Business Media, 2001. ISBN 978-3-642-63214-3. Dostupné z: <https://doi.org/10.1007/978-3-642-56853-4>. [cit. 2025-03-01].
- [50] NASA. *The Electromagnetic Spectrum*. Online. In: My NASA Data. 2004. Dostupné z: <https://mynasadata.larc.nasa.gov/basic-page/electromagnetic-spectrum-diagram>. [cit. 2025-02-27].
- [51] WORSFOLD, P.J. SPECTROPHOTOMETRY | Overview. Online. *Encyclopedia of Analytical Science*. 2005, s. 318-321. ISBN 9780123693976. Dostupné z: <https://doi.org/10.1016/B0-12-369397-7/00714-7>. [cit. 2025-01-19].
- [52] NNACHI ALUM, Benedict. Advances in UV Spectroscopy for Monitoring the Environment. Online. *Research invention journal of biological and applied sciences*. 2024, s. 82-89. Dostupné z: [https://www.researchgate.net/publication/381650499\\_Advances\\_in\\_UV\\_Spectroscopy\\_for\\_Monitoring\\_the\\_Environment](https://www.researchgate.net/publication/381650499_Advances_in_UV_Spectroscopy_for_Monitoring_the_Environment). [cit. 2025-03-30].
- [53] HUNTERLAB. *UV-VIS Spectroscopy for Water Analysis and Environmental Applications*. Online. 2023. Dostupné z: <https://www.hunterlab.com/blog/uv-vis-spectroscopy-for-water-analysis-and-environmental-applications.com>. [cit. 2025-03-30].

- [54] SHEIKH WAJIHA SHABBIR a SHILPI CHAUHAN. A REVIEW ON USE OF ULTRAVIOLET SPECTROSCOPY. Online. *Innovare Journal of Medical Sciences*. 2024, s. 5-11. ISSN 2321-4406. Dostupné z: <https://doi.org/10.22159/ijms.2024v12i4.51499>. [cit. 2025-03-30].
- [55] MEASURLABS. *A simplified diagram of the UV-vis system*. Online. In: . 2025. Dostupné z: <https://measurlabs.com/methods/uv-visible-spectroscopy/>. [cit. 2025-03-30].
- [56] HAKIM, Supwatul; WAHYUNINGSIH MANURUNG, Tety; HERMAYANTINGSIH, Dwi a ARIEFIN, Mokhamat. Electrochemical Oxidation of Methylene Blue Using Carbon Electrode from Battery Waste. Online. *Helium: Journal of Science and Applied Chemistry*. 2024, vol. 04, no. 02, s. 33-38. ISSN 2776-4508. Dostupné z: [https://www.researchgate.net/publication/387442083\\_Electrochemical\\_Oxidation\\_of\\_Methylene\\_Blue\\_Using\\_Carbon\\_Electrode\\_from\\_Battery\\_Waste](https://www.researchgate.net/publication/387442083_Electrochemical_Oxidation_of_Methylene_Blue_Using_Carbon_Electrode_from_Battery_Waste). [cit. 2025-03-31].
- [57] GOREN, Aysegul Yagmur; RECEPOĞLU, Yaşar Kemal; EDEBALI, Özge; SAHIN, Cagri; GENISOGLU, Mesut et al. Electrochemical Degradation of Methylene Blue by a Flexible Graphite Electrode: Techno-Economic Evaluation. Online. *ACS Omega*. 2022, roč. 7, č. 36, s. 32640-32652. ISSN 2470-1343. Dostupné z: <https://doi.org/10.1021/acsomega.2c04304>. [cit. 2025-03-31].
- [58] SRIVASTAVA, Vishal; SINGH, Pravin K.; SRIVASTAVA, Arjita a SINGH, Praveen P. Synthetic applications of flavin photocatalysis: a review. Online. *RSC Advances*. 2021, roč. 11, č. 23, s. 14251-14259. ISSN 2046-2069. Dostupné z: <https://doi.org/10.1039/D1RA00925G>. [cit. 2025-03-31].
- [59] IVANOVÁ, Lucia. *Synthesis and application of nature-inspired materials for photocatalytic processes*. Doctoral Thesis. Brno: Brno University of Technology, Chemical Faculty, Institute of Chemistry and Technology of Environmental Protection, 2024.
- [60] ČIČATKOVÁ, Dominika. *Author's own photos*.
- [61] HASONĚ, Stanislav; OSTATNÁ, Veronika a FOJTA, Miroslav. Simultaneous voltammetric determination of free tryptophan, uric acid, xanthine and hypoxanthine in plasma and urine. Online. *Electrochimica Acta*. 2020, roč. 329. ISSN 00134686. Dostupné z: <https://doi.org/10.1016/j.electacta.2019.135132>. [cit. 2025-02-04].
- [62] YAN, Fei; ERDEM, Arzum; MERIC, Burcu; KERMAN, Kagan; OZSOZ, Mehmet et al. Electrochemical DNA biosensor for the detection of specific gene related to *Microcystis* species. Online. *Electrochemistry Communications*. 2001, roč. 3, č. 5, s.

224-228. ISSN 13882481. Dostupné z: [https://doi.org/10.1016/S1388-2481\(01\)00149-7](https://doi.org/10.1016/S1388-2481(01)00149-7). [cit. 2025-04-11].

## 7. LIST OF ABBREVIATIONS

| <b>Abbreviation/symbol</b>    | <b>Meaning</b>                               |
|-------------------------------|--|
| MPs                           | micropollutants                              |
| WWTPs                         | wastewater treatment plants                  |
| PE                            | population equivalent                        |
| AOPs                          | advanced oxidation processes                 |
| AO                            | anodic oxidation                             |
| CO <sub>2</sub>               | carbon dioxide                               |
| H <sub>2</sub> O              | water  |
| BOD <sub>5</sub>              | biochemical oxygen demand                    |
| TOC                           | total organic carbon                         |
| N <sub>total</sub>            | total nitrogen                               |
| P <sub>total</sub>            | total phosphorus                             |
| PPCPs                         | pharmaceuticals and personal care products   |
| ROS                           | reactive oxygen species                      |
| •OH                           | hydroxyl radicals                            |
| H <sub>2</sub> O <sub>2</sub> | hydrogen peroxide                            |
| POPs                          | persistent organic pollutants                |
| UV                            | ultraviolet                                  |
| TiO <sub>2</sub>              | titanium dioxide                             |
| EAOPs                         | electrochemical advanced oxidation processes |
| COD                           | chemical oxygen demand                       |
| O <sub>2</sub> <sup>-•</sup>  | superoxide radical                           |
| ROO•                          | peroxyl radical                              |
| O <sub>2</sub>                | oxygen                                       |
| O <sub>3</sub>                | ozone  |
| Fe <sup>2+</sup>              | iron(II)                                     |
| RF                            | riboflavin                                   |
| Fe <sup>3+</sup>              | iron(III)                                    |
| Ar                            | argon  |
| N <sub>2</sub>                | nitrogen                                     |
| H <sup>+</sup>                | hydrogen ion                                 |
| Na <sup>+</sup>               | sodium cation                                |

|                               |  |
|-------------------------------|--|
| Cl <sup>-</sup>               | chloride anion                         |
| GC                            | glassy carbon                          |
| CPEs                          | carbon paste electrodes                |
| PGEs                          | pencil graphite electrodes             |
| PG                            | pencil graphite                        |
| BDD                           | boron-doped diamond                    |
| CH <sub>4</sub>               | methane                                |
| H <sub>2</sub>                | hydrogen                               |
| B <sub>2</sub> H <sub>6</sub> | diboran                                |
| $q_e$                         | charge on the electrode                |
| $q_s$                         | charge from the solution               |
| IHP                           | inner Helmholtz plane                  |
| OHP                           | outer Helmholtz plane                  |
| h <sup>+</sup>                | hole                                   |
| M                             | anode surface                          |
| e <sup>-</sup>                | electron                               |
| $E$                           | potential                              |
| $I$                           | current                                |
| $t$                           | time                                   |
| HPLC                          | High Performance Liquid Chromatography |
| CV                            | cyclic voltammetry                     |
| $E^0$                         | standard potential of a species        |
| F                             | Faraday's constant                     |
| $n$                           | number of electrons                    |
| $T$                           | absolute temperature                   |
| R                             | universal gas constant                 |
| SWV                           | Square wave voltammetry                |
| $E_{sw}$                      | square wave amplitude                  |
| $\Delta E_{sw}$               | step height                            |
| $\tau$                        | square wave period                     |
| $T_d$                         | delay time                             |
| CPE                           | controlled potential electrolysis      |
| EMR                           | electromagnetic radiation              |
| $\lambda$                     | wavelength                             |
| $\nu$                         | frequency                              |

|                                |   |
|--------------------------------|---|
| $c$                            | speed of light in vacuum  |
| $h$                            | Planck's constant   |
| UV-VIS                         | ultraviolet-visible   |
| IR                             | infrared  |
| $A$                            | absorbance  |
| $d$                            | path length   |
| $\epsilon$                     | extinction coefficient  |
| VIS                            | visible   |
| MB                             | Methylene bBlue   |
| FLs                            | flavins   |
| A-Na-TEG                       | 1,3-bis(2-(2 (2methoxyethoxy)ethoxy)ethyl)naphtho[2,3g]pteridine-2,4(1H,3H)-dione |
| Ag/AgCl                        | silver/silver chloride  |
| NaCl                           | sodium chloride   |
| OCC                            | open-circuit conditions   |
| H <sub>3</sub> PO <sub>4</sub> | phosphoric acid   |
| GrO                            | graphite oxides   |
| $C$                            | electrode double layer,   |
| ac                             | alternating current   |
| SEM                            | scanning electron microscopy  |
| XPS                            | X-ray photoelectron spectroscopy  |
| LMW                            | low-molecular-weight  |
| $Q$                            | total charge  |
| MS                             | Mass Spectrometry   |